# Sequence stratigraphic framework of carbonates in mixed siliciclastic–carbonate sequences: local versus external controls in a tectonically active basin (Lorca Basin, Miocene, SE Spain)

Cédric Carpentier, Emmanuelle Vennin, Nicolas Olivier, Bertrand Martin-Garin

# SEQUENCE STRATIGRAPHIC FRAMEWORK OF CARBONATES IN MIXED SILICICLASTIC–CARBONATE SEQUENCES: LOCAL *VERSUS* EXTERNAL CONTROLS IN A TECTONICALLY ACTIVE BASIN (LORCA BASIN, MIOCENE, SE SPAIN)

CÉDRIC CARPENTIER,[1] EMMANUELLE VENNIN,[2] NICOLAS OLIVIER,[3] AND BERTRAND MARTIN-GARIN[4]

[1]*Université de Lorraine, CNRS, GeoRessources, 54000 Nancy, France*

[2]*Biogéosciences, UMR 6282 CNRS, Université Bourgogne, 6 Boulevard Gabriel, 21000 Dijon, France*

[3]*Université Clermont Auvergne, CNRS, IRD, OPGC, Laboratoire Magmas et Volcans, 63000 Clermont-Ferrand, France*

[4]*Aix Marseille Univ, CNRS, IRD, INRAE, CEREGE, Marseille, France*

*e-mail: cedric.carpentier@univ-lorraine.fr*

**ABSTRACT:**

**The sequence stratigraphic framework of initiation and growth of carbonates in environments impacted by siliciclastic inputs is highly variable because of the biogenic nature of the sedimentary production and its sensitivity to environmental conditions. Using panorama interpretations, logging, and characterization of benthic communities, the mixed carbonate–siliciclastic sedimentary succession of the Neogene Lorca Basin (SE Spain) has been studied to decipher the role of local and global controlling parameters on the sequence stratigraphic framework of carbonate production. Three different carbonate depositional models are distinguished: 1) retrogradational homoclinal ramps (type 1) dominated by heterozoan communities that developed lateral to alluvial fans, 2) progradational flat-topped coral platforms (type 2) with *Porites* and *Tarbellastraea* coral carpets with a coeval retrogradational pattern on basin margins, and 3) retrogradational narrow siliciclastic-rich coral platforms (type 3) with *Tarbellastraea* buildups intercalated with deltaic deposits. Onset of carbonate production systematically occurred during transgressions controlled by eustasy and was locally enhanced by extensional tectonics. In steep margins located in the vicinity of major marginal faults, transgressions were characterized by high terrigenous inputs, and only heterozoan-dominated ramps (type 1) developed. The flooding of these steep and tectonically active margins characterized by small drainage basins and immature, locally sourced alluvial systems led to lower terrigenous fluxes and the growth of coral flat-topped platforms (type 2) during subsequent highstands. Away from main marginal faults, deltaic environments were sourced by large drainage basins. They were characterized by a flat topography that permitted the occurrence of a shallow photic zone subject to low and irregular terrigenous inputs up to the distal part of the depositional profile during transgressions. In this deltaic configuration, the growth of narrow siliciclastic-rich coral platforms (type 3) were favored. On these platforms, coral buildups were regularly buried by terrigenous inputs during highstands. In the Lorca Basin, the dimensions of siliciclastic systems and the size of their drainage basins also directly impacted the sequence stratigraphic framework of carbonates intercalated in terrigenous units. This study illustrates the marked variability in: 1) the different types of carbonate depositional profiles and 2) the timing of these carbonates in a mixed carbonate–siliciclastic system because of the size, maturity, and location of siliciclastic systems, local tectonics, inherited topography, and global sea-level fluctuations.**

## INTRODUCTION

Numerous studies have been published about the sequence stratigraphic framework of carbonate deposits in mixed siliciclastic–carbonate systems (Coffey and Read 2004; Bassant et al. 2005; Garcia-Garcia et al. 2006; Reuter and Brachert 2007; Bauch et al. 2011; Corrochano et al. 2012; Tomassetti and Brandano 2013; D'Agostini et al. 2015; Zeller et al. 2015; Zecchin and Catuneanu 2017; Schwarz et al. 2018; Daniell et al. 2020). All these studies demonstrate that the sequence stratigraphic framework for the initiation and expansion of carbonate production is highly variable and as stated by Zecchin and Catuneanu (2017) "*The marked variability of mixed siliciclastic–carbonate sequences makes the definition of a universal sequence stratigraphic model impossible* . . .". Indeed, carbonate production due to its biogenic origin is largely dependent on environmental parameters, and therefore its controlling factors are multiple and complex (Kiessling et al. 2003; Pomar et al. 2004; Schlager 2005; Wright and Burgess 2005; Pomar and Hallock 2008; Michel et al. 2018; Reijmer 2021). Variations in one or more environmental parameters can lead to modifications in benthic associations, and in the volume of carbonate production (Isern et al. 1996; Riegl 2001; Mutti and Hallock 2003; Lukasik and James 2006; Chazottes et al. 2008; Schäfer et al. 2011; Paul et al. 2012) that can induce changes in the geometry of carbonate systems (Pomar 2001; Schlager 2003; Betzler et al. 2012; Pomar et al. 2012). Drastic environmental changes can result in a

critical decrease in carbonate production or even to the demise of the carbonate systems (Hallock and Schlager 1986; Philip and Airnaud-Crumière 1991; Isern et al. 1996; Carpentier et al. 2010; Bauch et al. 2011; Rosleff-Soerensen et al. 2012; Masse and Fenerci-Masse 2013). At basin scale, tectonics, eustasy, and climate are the main factors controlling environmental changes such as water depth, light, terrigenous and nutrient inputs, temperature, $pCO_2$, basin physiography, salinity, oxygenation, and substrate (Martin-Chivelet 1995; Wilson and Lokier; 2002; Olivier et al. 2004, 2015; Vecsei 2004; Webster et al. 2004; Bosence 2005; Schlager and Warrlich 2009; Bauch et al. 2011; Martin-Garin et al. 2012; Navarrete et al. 2013; Martin-Garin and Montaggioni 2023). Local processes such as lateral shifts of areas of terrigenous input may also impact the benthic communities and therefore carbonate production (Pratt and James 1986; Heap et al. 2002; Schwarz et al. 2018). As a consequence, a direct application of Walther's law during an entire transgression–regression cycle is not realistic in mixed systems (Homewood 1996; Wright and Burgess 2005). Then, deciphering the impact of these different factors on the production of carbonates and development of benthic communities in a basin prone to important terrigenous inputs is a challenge and contributes to our understanding of the sequence stratigraphy in mixed carbonate–siliciclastic depositional systems.

The Neogene basins of the Betic Cordillera were tectonically active during the Tortonian and the Messinian, and recorded alternations of carbonate and siliciclastic units (Sanz de Galdeano and Vera 1992; Montenat et al. 1996; Bourillot et al. 2009, 2010; Rodriguez-Fernandez et al. 2012). Thus, the nature and evolution of carbonate deposits of the Betics have been widely studied in the majority of these intramountain and marginal basins (Braga and Martin 1988, 1996; Saint-Martin and Rouchy 1990; Franseen and Mankiewicz 1991; Martin et al. 1996; Betzler et al. 1997; Brachert et al. 2001, 2002; Braga and Aguirre 2001; Braga et al. 2001, 2006; Vennin et al. 2004; Johnson et al. 2005; Warrlich et al. 2005; Garcia-Garcia et al. 2006; Puga-Bernabéu et al. 2007, 2014; Bourillot et al. 2010). However, the Lorca Basin, characterized by a complex sedimentary infill with rapid lateral shifts of facies and thickness variations, has been poorly studied. Apart from paleoecological and sedimentological studies focused on local outcrops (Vennin et al. 2004; Thrana and Talbot 2006; Sælen et al. 2016) or on the Messinian series (Rouchy et al. 1998; Wrobel and Michalzik 1999; Carpentier et al. 2020), the modalities of the onset, development, and demise of carbonate systems, and their spatial and temporal relationships with terrigenous sedimentation, have never been clearly described.

By means of detailed geological mapping, panorama interpretations, sedimentary logging, facies analysis, study of biotic assemblages, and sequence stratigraphy, this paper aims to: 1) characterize carbonate depositional models in a basin impacted by significant terrigenous input, 2) determine the sequence stratigraphic framework of the carbonate production for each model, and 3) decipher the role of controlling factors including local tectonics, topography, size of the drainage basins, and eustasy on the biotic assemblages, the volume and the location of entry points of siliciclastic sediments in the basin, and the sequence stratigraphic framework of carbonate production.

## GEOLOGICAL FRAMEWORK

The Betic Cordillera, located in southeastern Spain, is oriented ENE–WSW (Fig. 1A). This orogenic complex, along with the Rif Mountains in Morocco, is part of the Gibraltar arc and was created by the convergence of the Iberian and African plates (Dercourt et al. 1986). The Guadalquivir Basin, located to the northwest, corresponds to the foreland basin between the external Betics, characterized by folded and thrusted Mesozoic and Neogene sediments, and the Iberian platform (Frizon de Lamotte et al. 1989; Cloetingh et al. 1992; Sanz de Galdeano and Vera 1992; Galindo-Zaldivar et al. 1993; Riaza and Martinez del Olmo 1996; Iribarren et al. 2007) (Fig. 1B). The widest expanse of the Alboran crustal domain is located offshore between Spain and Morocco, and the internal Betics represent its terrestrial continuation (Comas et al. 1992; Sanz de Galdeano and Vera 1992; Iribarren et al. 2007; Platt 2007) (Fig. 1B). The internal Betics consist of sierras of metamorphic rocks separated by narrow basins filled by Neogene sediments (Sanz de Galdeano 1990; Montenat 1996; Meijninger and Vissers 2006) (Fig. 1C). The Lorca Basin is one such basin, bounded to the southeast by the strike-slip Alhama de Murcia Fault (AMF) and the Sierra de la Tercia, while its northwestern margin goes beyond the Internal–External Zone boundary (Guillen Mondejar et al. 1995; Montenat and Ott d'Estevou 1996, 1999; Booth-Rea et al. 2002; Martinez-Diaz 2002; Meijninger and Vissers 2006) (Fig. 1C). The existence of a major NE–SW fault in the center of the basin, named the Falta Central de la Cuenca de Lorca (FCCL, Fig. 1D), has been inferred by several authors (Guillen Mondejar et al. 1995; Meijninger and Vissers 2006). The outcrops on which this study is based are located on the southwestern margin of the basin, where Tortonian–Messinian formations are well exposed. They are crosscut by faults, such as the NW–SE Batanes Fault, which bounds carbonate units to the east (Guillen Mondejar et al. 1995; Montenat and Ott d'Estevou 1999; Vennin et al. 2004) (Fig. 1D).

The origin and geodynamic evolution of the Neogene basins of the Betics are still debated. Most of them were firstly interpreted as pull-apart or "groove-shaped synclines" formed in a compressional context from the early or middle Miocene until present because of the occurrence of strike-slip faults at their edges (Cloetingh et al. 1992; Montenat and Ott d'Estevou 1996, 1999). More recently, some authors proposed that most of the Neogene basins were formed during the collapse of the Alboran domain and the exhumation of metamorphic complexes (Booth-Rea et al. 2004; Augier et al. 2005; 2013; Do Couto et al. 2014, 2016). In such a context, these basins were controlled by high-angle normal faults in the brittle domain above detachment planes (Chalouan et al. 1997; Booth-Rea et al. 2004; Augier et al. 2005, 2013; Rodriguez-Fernandez et al. 2012; Do Couto et al. 2014, 2016; Giaconia et al. 2014). These authors consider that the main NE–SW strike-slip faults (Carboneras, Palomares, and Alhama de Murcia faults, Fig. 1C) first acted as normal or transfer faults (Martinez-Martinez et al. 2006; Meijninger and Vissers 2006; Rodriguez-Fernandez et al. 2012; Giaconia et al. 2014) and that strike-slip movement began only during the late Tortonian or the early Messinian (Booth-Rea et al. 2003; Giaconia et al. 2012; Augier et al. 2013). In the Lorca Basin, a synsedimentary Serravalian to late Tortonian NE-directed extensional activity was evidenced by Meijninger and Vissers (2006), while the strike-slip motion along the Alhama de Murcia Fault that generated the uplift of the Sierra de la Tercia is supposed to have started during the early Messinian.

## STRATIGRAPHIC FRAMEWORK

The Tortonian and Messinian formations on the southwestern margin of the Lorca Basin consist of an alternation of carbonate and siliciclastic deposits. Because of rapid lateral changes in facies, the stratigraphic framework can be subdivided in two stratigraphic columns for the Los Arcos–Las Canteras and Los Cautivos areas (Fig. 2 and location in Fig. 1D).

### *Los Arcos–Las Canteras Area*

The earliest Tortonian sediments consist of marine marls, sandstones, and limestones of the lower part of the Parilla Formation (Fm) (Sælen et al. 2016; Vennin et al. 2004) (Fig. 2). The studied stratigraphic interval concerns the Enamorados Limestones Member (Mbr) corresponding to the upper part of the Parilla Fm. The lower part of the Enamorados Limestones Mbr consists of calcarenites rich in foraminifers (mainly

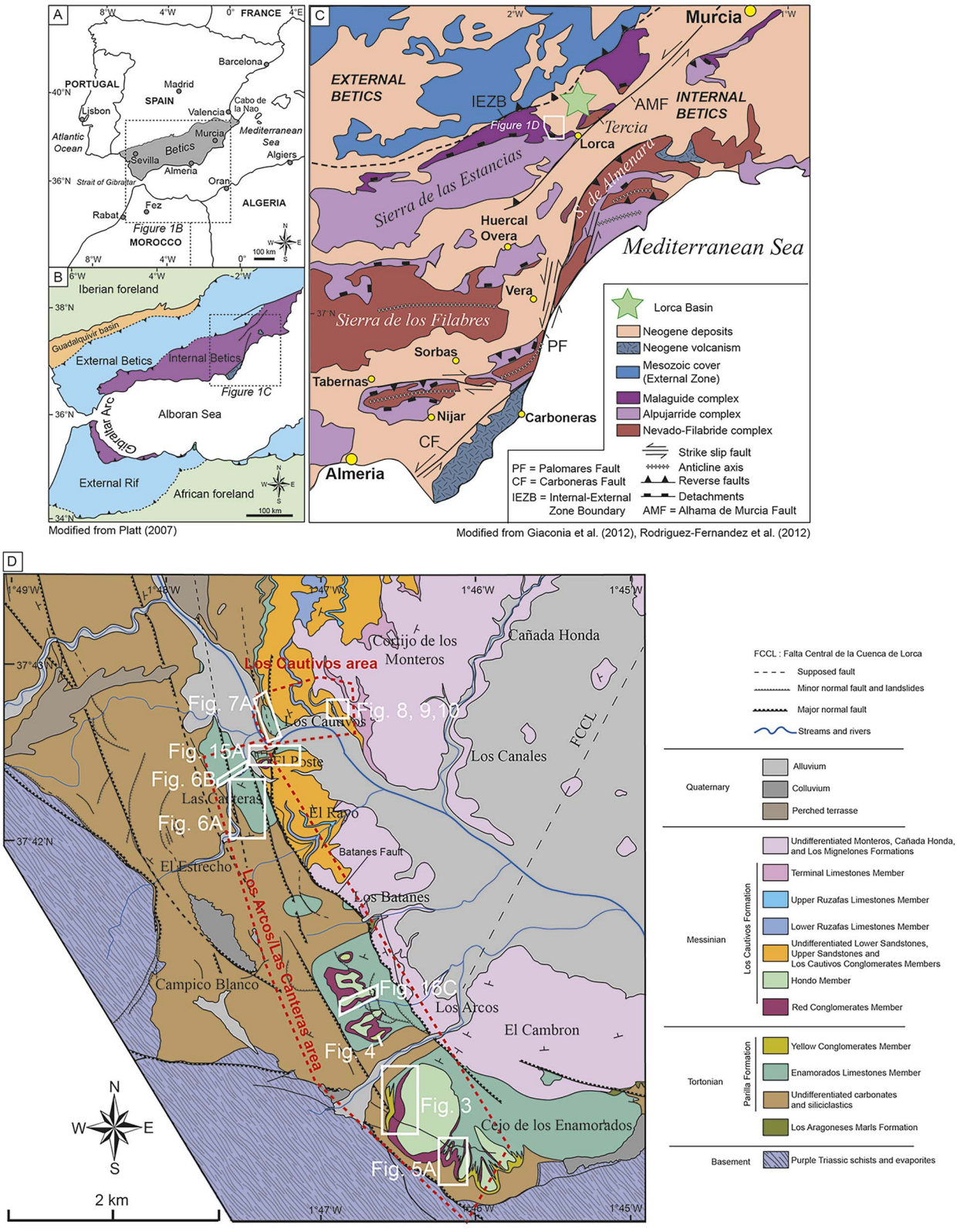


FIG. 1.—Location and geological maps of the study area. **A)** Location map of the Betic Cordillera. **B)** Structural units of the Alboran and Betics domains. **C)** Geological map of the main Neogene basins and tectonic structures of the Internal Betics. **D)** Geological map of the study area in the southwestern part of the Lorca Basin with locations of figures with field observations.

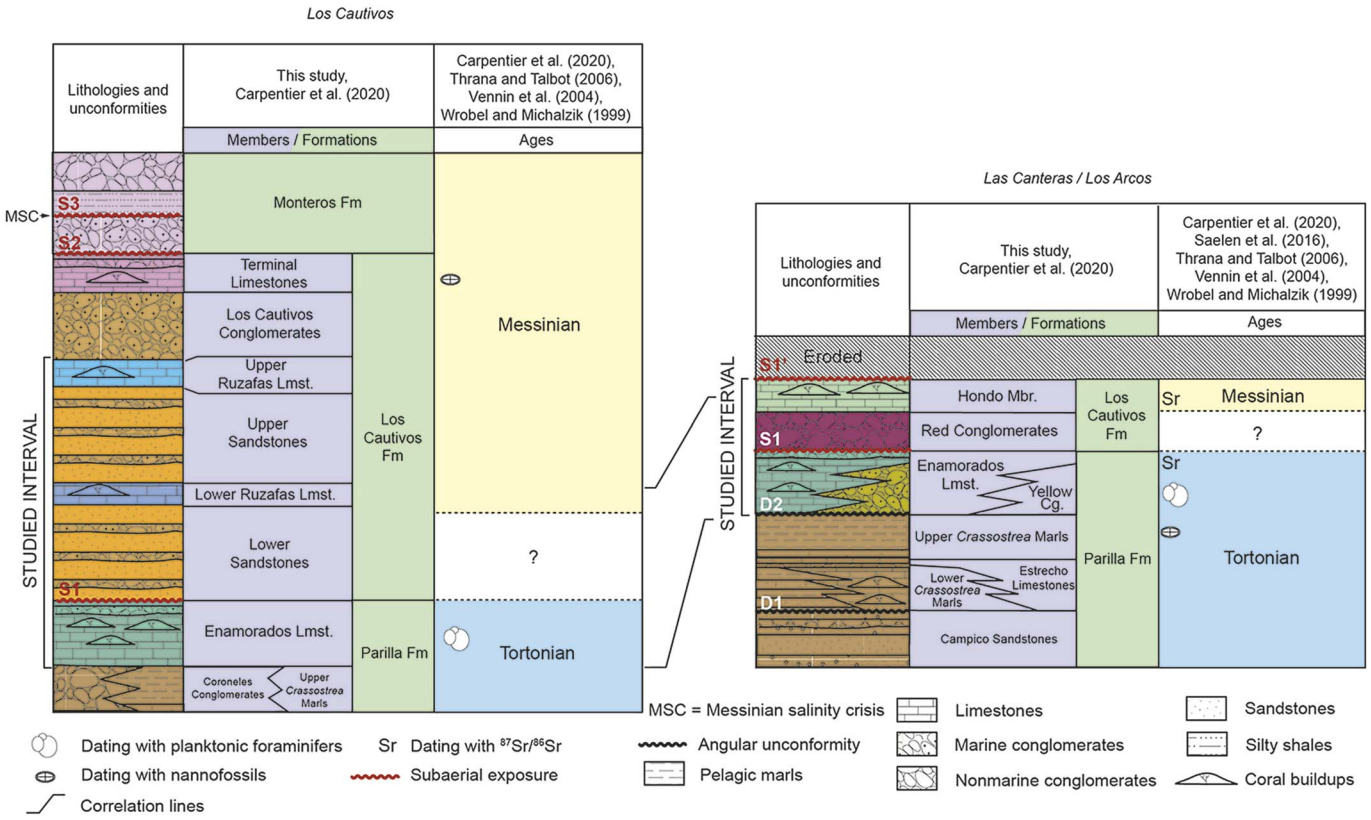


FIG. 2.—Stratigraphy of the southwestern Lorca Basin in the Los Arco–Las Canteras and Los Cautivos areas (locations on Fig. 1D).

*Heterostegina*), and the upper part is composed of *Porites*- or *Tarbellastraea*-rich carbonates. The basal surface of the Enamorados Limestones Mbr corresponds to an angular unconformity (D2 unconformity). The study of nannofossils in the Upper *Crassostrea* Marls Mbr located below the D2 unconformity revealed the occurrence of *Amaurolithus primus*, suggesting a late Tortonian age (Carpentier et al. 2020). The Enamorados Limestones grade laterally to marine siliciclastics of the Yellow Conglomerates Mbr. The Red Conglomerates Mbr overlies a surface of subaerial exposure (S1) on the top of the Enamorados Limestones (Vennin et al. 2004) (Fig. 2). These conglomerates are overlain by carbonates of the Hondo Mbr that are topped by a surface of subaerial exposure S1′ (Vennin et al. 2004). Based on Sr isotopes, Sælen et al. (2016) placed the Tortonian–Messinian boundary between the Enamorados Limestones and Hondo mbrs.

### *Los Cautivos Area*

The studied stratigraphic interval includes upper Tortonian and Messinian deposits that predate the Messinian Salinity Crisis (MSC, Fig. 2) and the deposition of evaporites in the central part of the basin (Wrobel and Michalzik 1999; Carpentier et al. 2020). The studied deposits correspond to the upper part of the Parilla Fm (Enamorados Limestones Mbr) and the Los Cautivos Fm. It consists of an alternation of conglomeratic and sandy units and calcarenitic carbonates rich in *Tarbellastraea* and *Porites* corals. Siliciclastic deposits correspond to the Lower and Upper Sandstones, and Los Cautivos Conglomerates Mbrs (Carpentier et al. 2020). Carbonates correspond to the Enamorados Limestones and the Lower and Upper Ruzafas Limestones Mbrs. The Enamorados Limestones are topped by the erosional surface of subaerial exposure S1. Despite the lack of continuous outcrop between localities, stratigraphic successions suggest that the Lower Ruzafas Limestones correspond to the lateral equivalent of the Hondo Mbr in the Los Arcos area (locations in Fig. 1D). A Messinian age was proposed for the Los Cautivos Fm by Wrobel and Michalzik (1999) based on foraminifera assemblages (Upper pre-evaporitic unit of Wrobel and Michalzik 1999). Nannofossils indicate a Messinian age for the Terminal Limestones Mbr that are capped by the incision surface S2 (Carpentier et al. 2020). The upper part of the Messinian interval corresponds to the Monteros Fm, which is characterized by alternations of marls, sandstones, and conglomerates crosscut by the incision surface S3 related to the Messinian Salinity Crisis.

## MATERIAL AND METHODS

Detailed geological mapping was performed to describe the lateral variations of facies. Panoramas were interpreted to identify sedimentary geometries, unconformities, and the chronology of faults. Laterally continuous outcrops made it possible to follow the lateral evolution of benthic communities along depositional profiles. Facies were interpreted in terms of depositional environments based on sedimentary structures, geometries of sedimentary bodies, biotic assemblages, and petrography. The petrography and depositional environments were complemented by the study of microfacies using optical microscopy on thin sections with an Olympus BX51 microscope equipped with a Zeiss AxioCam ICc 1 camera. Amounts of siliciclastics in carbonate facies were estimated optically on the field for the coarser fraction (gravels to pebbles) and on thin sections by using an optical chart for the fine-grained fraction. The study of panoramas was systematically coupled with the logging of several sedimentary successions to characterize the vertical and lateral evolution of facies and to refine the sequence stratigraphic interpretation. Sedimentary geometries were interpreted in terms of progradation,

aggradation, and retrogradation due to the interplay between accommodation and flux of sediments (Emery and Myers 1996; Posamentier and Allen 1999). The terms sigmoid progradation and oblique progradation (*sensu* Catuneanu et al. 2009) are used to distinguish progradation with aggradation (positive accommodation) and progradation without aggradation (low or null accommodation), respectively.

## RESULTS

### *Stratigraphic Architecture and Facies Enamorados Limestones and Hondo Mbrs*

**Los Arcos.—**The edges of the NE–SW-oriented valley south of Los Arcos (location in Fig. 1D and Supplemental File S6) expose the geometries and the stratigraphic organization of the Enamorados Limestones, Red Conglomerates, and Hondo Mbrs. The Enamorados Limestones onlap the D2 angular unconformity (Fig. 3A). The stratigraphic architecture in this area has been studied by Thrana and Talbot (2006). They propose a lateral transition between the Red Conglomerates and the Enamorados Limestones. However, detailed mapping of the area shows that carbonates grade laterally into yellow marine sandstones and conglomerates of the Yellow Conglomerates Mbr and not into the Red Conglomerates (Fig. 3A, B). Because of the angular unconformity (D2) and the onlap geometry, the thickness of marine sandstones and conglomerates decreases gradually towards the basin margin to reach less than 3 m in the southwest (Fig. 3A, B). Basinward, the lateral transition between the yellow marine siliciclastics and the Enamorados Limestones is abrupt, and occurs over 50 to 150 m. Geometries at the outcrop scale (Fig. 3A) indicate a retrogradation of this carbonate–siliciclastic transition.

Facies in the lower part of the Enamorados Limestones are organized into metric stacked sequences (Fig. 4A) made of fine-grained calcarenites with planktonic foraminifera and rare coralline algae (Mr facies, Table 1) covered by medium- to coarse-grained calcarenites rich in *Heterostegina* and coralline algae (Ir facies, Table 1, Supplemental Fig. S1E). Corals are rare and appear only locally as small *Porites* buildups on top of sequences (Fig. 4A). The upper part of the Enamorados Limestones is also organized into metric stacked sequences (Fig. 4B). From base to top they are characterized by a fine-grained calcarenite (Ts facies, Table 1, Fig. S2J, K) grading upward into coral carpets of thin branching *Porites* embedded in a fine-grained calcarenite with reworked *Ostrea edulis* and thin *Porites* clasts (Ls facies, Table 1) (Fig. 4C). The top of sequences is made of deposits rich in closely spaced and thick robust branching *Porites* accompanied by disseminated massive forms (Fig. 4B) (Us, Pe facies, Table 1). Toward the basin margin, this facies grades laterally into a coarse-grained, rhodolith and siliciclastic-rich calcarenite with *in situ* buildups of massive domal *Tarbellatraea* and *Porites* locally (Op facies, Table 1). In the transition zone with Yellow Conglomerates, unsorted conglomeratic beds with bored pebbles (Ip facies, Table 1) are intercalated between coarse-grained calcarenites of the facies Op or basement pebble-rich calcarenites of the facies Ip (Table 1, Fig. S2A) (Fig. 3C). Yellow marine sandstones and conglomerates become dominant in the most proximal part. A sharp transition to coarse-grained calcarenites rich in siliciclastic gravels (Ip facies) occurs in the upper part of the Enamorados Limestones (Fig. 4A, D, Fig. S2B). In addition, the Enamorados Limestones are capped by the S1 surface of subaerial exposure showing karstic features (Vennin et al. 2004; Sælen et al. 2016) and directly overlain by unsorted conglomerates of the Red Conglomerates Mbr (Af facies, Table 1, Fig. S5A) (Fig. 3A). Clasts of these red conglomerates consist exclusively of Triassic metapelites and schists that constitute the neighboring substratum of the southern basin margin.

Carbonates of the Hondo Mbr rich in closely spaced *Tarbellastraea* buildups (Fig. 4E) cover the Red Conglomerates Mbr through a marine transgression surface, and conglomerates pinch out northeastward in a basinal direction (Fig. 3A). The geometries of the Hondo Mbr can be observed at the tops of several hills to the southeast of the Los Arcos Valley (Fig. 5, location in Fig. 1D). Deposits are characterized by northwestward-prograding geometries (Fig. 5A). On the formation-wide scale, offlap geometries represent an oblique progradation without aggradation in proximal parts of the profile.

Facies in the Hondo Mbr resemble those observed in the Enamorados Limestones Mbr. The marine transgression surface on top of the Red Conglomerates is covered by conglomerates embedded in a calcarenitic matrix rich in clasts of coralline algae (Ir facies, Fig. 5B). The content of siliciclastics decreases vertically, and the overlying fine-grained calcarenites are rich in *Crassostrea gryphoides* buildups, and are crosscut by erosional surfaces overlain by shell accumulations (Mr facies, Fig. 5C). This facies is lacking in most proximal parts of the profile toward the southeast, where calcarenites rich in coralline algae are directly covered by *Tarbellastraea* and *Porites* patches in a coarse-grained calcarenite (Section 3 in Fig. 5B). The prograding units record a vertical stacking of thin branching *Porites* in a fine-grained matrix (Ls facies) overlain by thick branching and domal *Porites* buildups (Us and Pe facies, Fig. 5B, C). Thin branching *Porites* appear in the distal part of flat foresets to the northwest (Fig. 5C). Conversely, *Tarbellastraea* are more abundant in the upper part of the prograding units, which are also characterized by siliciclastic sediments in a coarse-grained calcarenite rich in rhodoliths (Op facies). A surface of subaerial exposure (S1′) characterized by karstic features occurs at the top of the Hondo Mbr (Fig. 5C).

**Las Canteras.—**In the Las Canteras area (location in Fig. 1D), the Lower Crassostrea Marls Mbr, a lateral equivalent of the Estrecho Limestones Mbr, covers the Campico Sandstones through a first unconformity (D1). The Enamorados Limestones Mbr covers a second unconformity (D2) truncating the Upper *Crassostrea* Marls (Fig. 6A). These limestones are characterized by sigmoids 7–10m-high prograding to the NE (Fig. 6B).

The facies in prograding clinoforms are similar to those described in the Los Arcos area. Clinoforms show a vertical and lateral transition from fine-grained calcarenites (Ts facies, Fig. S2I)), through thin branching *Porites* carpets with rare *Acanthastraea* (Ls facies, Fig. S2G, H), thick robust branching *Porites* buildups (Us facies, Fig. S2E, F), domal and branching *Porites* buildups (Pe facies, Fig. S2D), to a coarse-grained calcarenites with siliciclastic gravels and *Tarbellastraea* buildups (Op facies) (Fig. 6B, C, Fig. S2C). Carbonates observed in the Las Canteras area are relatively poor in siliciclastics, with only scattered gravel-size terrigenous grains at the top of sigmoids and silt-size siliciclastic grains present in fine-grained calcarenites at the distal end. As in Los Arcos, a surface of subaerial exposure (S1 in this study) on top of the Enamorados Limestones was described by Vennin et al. (2004).

**Los Cautivos.—**In the Los Cautivos area, the Enamorados Limestones are exposed along the eastern side of the Guadalentine valley (Fig. 7A). They cover the Coroneles Conglomerates Mbr, which grades laterally southward to the Upper *Crassostrea* Marls (Fig. 2). Conglomerates show a north-to-south transition from clast-supported channelized and unsorted matrix-supported conglomerates to sheets of coarse-grained sandstones (Fig. 7A) (Mf facies, Table 1, Fig. S5B–D). This trend indicates a N–S to NW–SE direction of siliciclastic inputs in this area perpendicular to the progradation direction of carbonates. As in the overlying Enamorados Limestones Mbr, the terrigenous material is polygenic and contains clasts of basement, oolitic limestone, dolomite, sandstone, and calcarenite. It contrasts with basement-derived conglomerates of the Los Arcos–Las Canteras area. The Enamorados Limestones cover the conglomerates

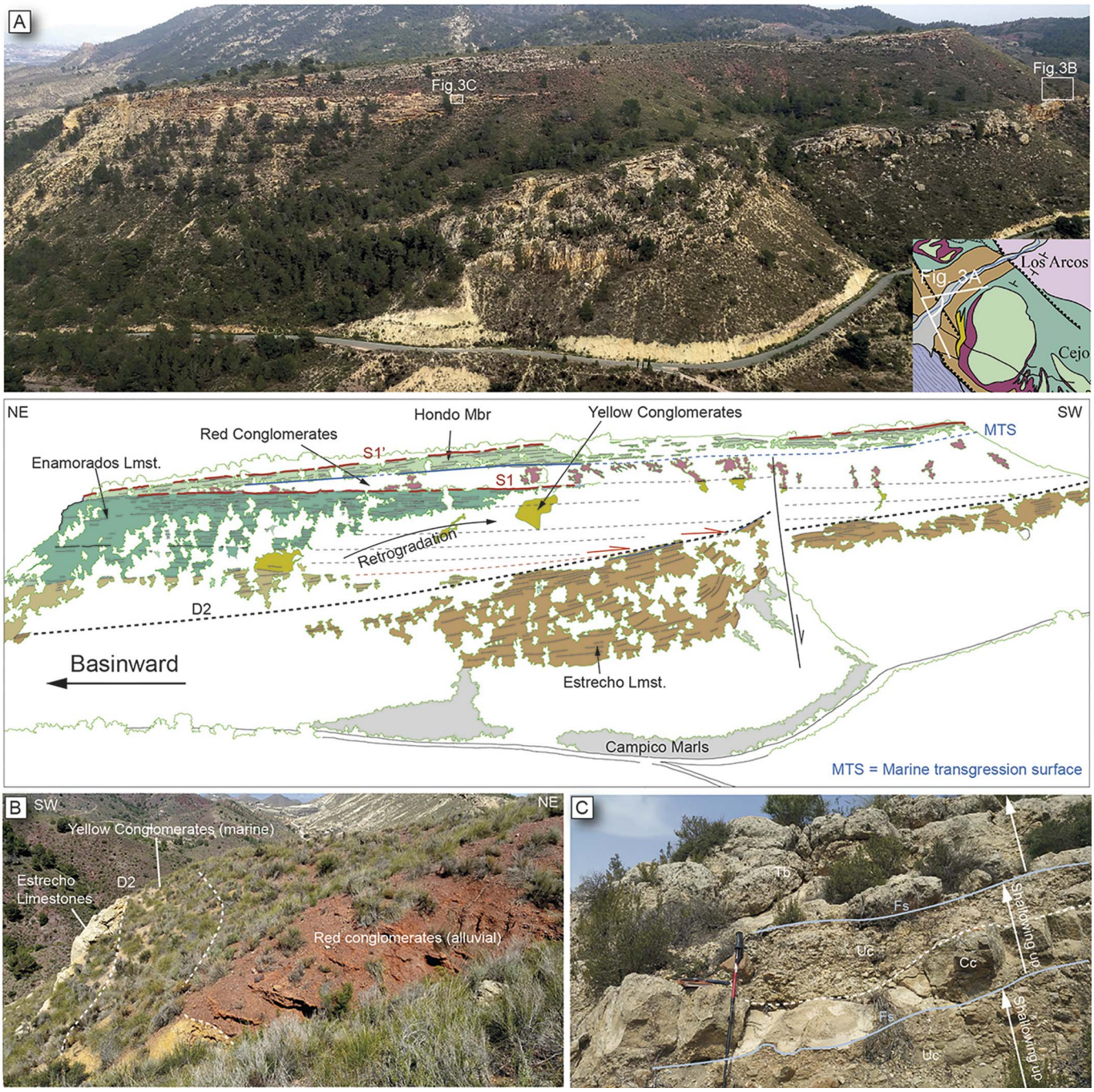


FIG. 3.—Stratigraphical and sedimentological features of the Enamorados Limestones Mbr on the southeastern side of the Los Arcos valley. **A)** Panorama of the southeastern side showing the geometrical relationships between carbonate units, siliciclastics, and D2 unconformity. **B)** Yellow marine sandstones and conglomerates covering the D2 unconformity in proximal parts of the depositional profile. They grade basinward to the Enamorados Limestones Mbr, topped by S1 karstified surface and are overlain by red conglomerates deposited in an alluvial fan environment. **C)** Facies stacking in inner-platform environment made of an alternation of marine conglomerates (Uc), coarse-grained calcarenites (Cc), and *Tarbellastraea* buildups (Tb) organized in shallowing-upward sequences bounded by flooding surfaces (Fs).

through a sharp surface (D2), but the angular unconformity is not well marked in this area.

First, carbonate deposits consist of the stacking of calcarenites with conglomeratic ribbons covered by fine-grained calcarenites rich in coralline algae (Ir facies) (Fig. 7B). Bioerosion is important in polygenic conglomerates, and the fauna is dominated by *in situ* suspension-feeding organisms such as barnacles and encrusting oysters (Fig. 7C). The Enamorados Limestones Mbr is characterized by the vertical stacking of high-frequency sequences (Fig. 7D). The lower part of the member is dominated by alternations of the Ls facies and *Porites*-rich deposits of the Us, Pe, and Op facies (Fig. 7D) and by an enlargement of the carbonate sedimentation zone to the north, where it grades laterally into marine conglomerate deposits (Ip facies) (Fig. 7A). The upper part of the member shows a gradual enrichment in conglomerates (Ip facies) and the disappearance of fine-grained calcarenites (Ls facies) (Fig. 7D). The top of the carbonates is truncated by an incision surface (S1). The incision is filled by cross-stratified, nonmarine, clast-

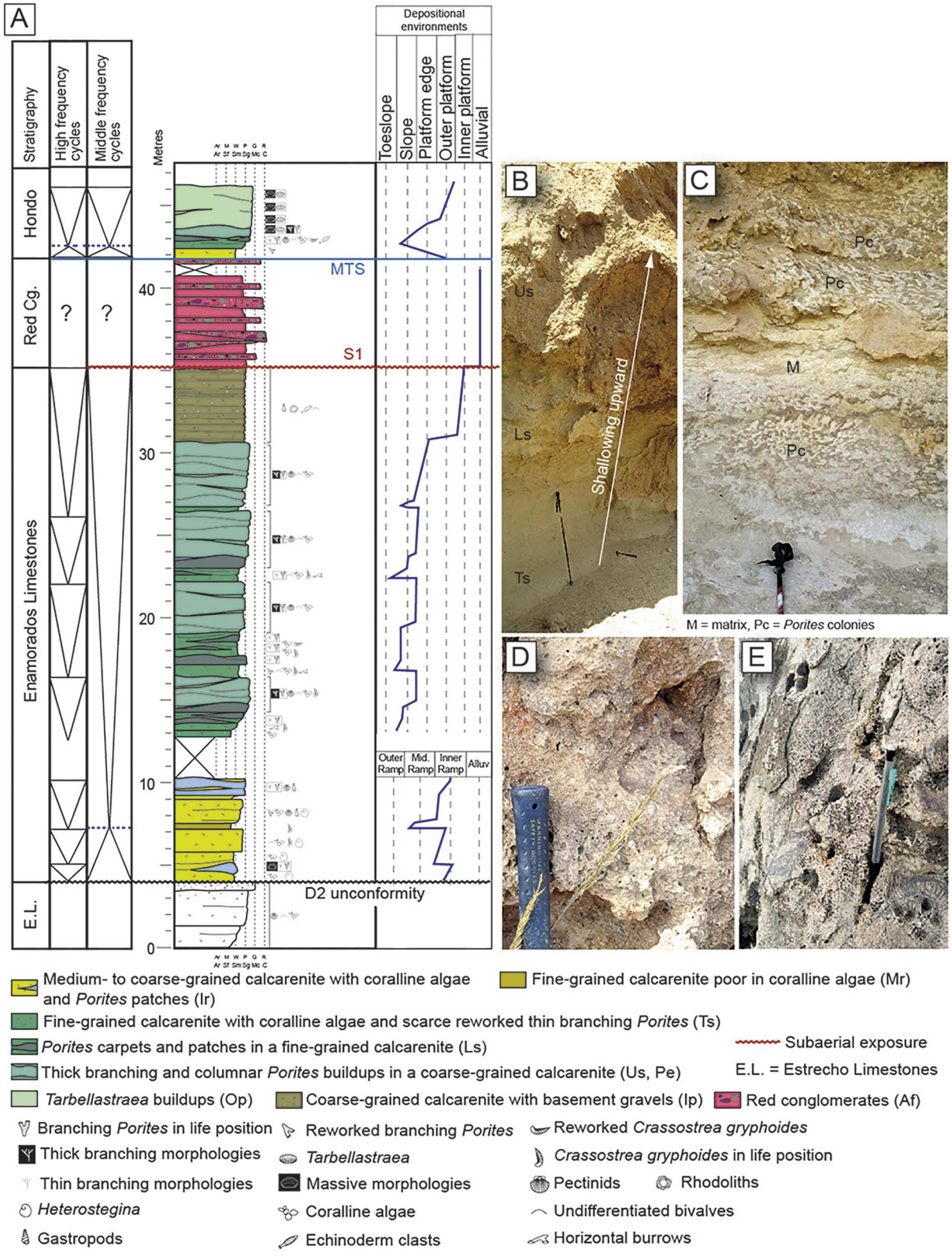


FIG. 4.—Log and sedimentological features of the Enamorados Limestones Mbr on the northern side of the Los Arcos valley. **A)** General log of the northern side of the Los Arcos valley with the interpretation of depositional environments and deduced sequence-stratigraphic evolution. **B)** Shallowing-upward high-frequency sequence in the Enamorados Limestones Mbr. Toeslope facies (Ts) are represented by non-bioturbated or bioturbated fine-grained calcarenite. Thin branching *Porites* carpets or buildups (Ls) indicate the transition to the lower-slope environment and the thick branching *Porites* (Us) mark upper-slope. **C)** Detail of thin branching *Porites* buildups (Ls). **D)** Coarse-grained and siliciclastics-rich calcarenite (Ip) in the upper part of the Enamorados Limestones Mbr. **E)** Closely spaced structure of *Tarbellatraea* buildup of the Op facies in the Hondo Mbr.

TABLE 1.—*Facies table.*

| Facies Associations | Lithology | Siliciclastic Content | Geometry | Sedimentary Structures and Spatial Facies Distribution | Biogenic Structures | Biotic Content | Interpretations |
|---|---|---|---|---|---|---|---|
| **Carbonates** | | | | | | | |
| *Los Arcos/Las Canteras* | | | | | | | |
| **Homoclinal Ramp (Depositional Profile 1)** Enamorados Limestones and Hondo Mbr | | | | | | | |
| **Ir** (Fig. S1A–E, Supplemental material) | Clast- or matrix-supported conglomerates with basement pebbles. Coarse-grained calcarenite with rhodoliths, *Heterostegina* grainstone | 85% | Horizontal stratifications | Basinward transition from conglomerates to a coarse-grained calcarenite with rhodoliths and rare corals and to *Heterostegina* grainstones | *Gastrochaenolites*, small coral patches several meters in width and tens of centimeters in thickness | *Ostrea edulis*, alveolinids, miliolids, ostracods. Encrusting lamellar or massive *Tarbellastraea* and *Porites*. *Heterostegina* foraminifera, bivalves, echinoderms, clasts of coralline algae or rhodoliths | **Inner-ramp.** Impacted by debris-flows. Agitated environment above the fair-weather wave base and transition to *Heterostegina* shoal in the distal part of the inner-ramp (Burchette and Wright 1992). |
| **Mr** (Fig. S1F, Supplemental material) | Medium- to fine-grained calcarenites rich in terrigenous grains and shell accumulations | 6% | Horizontal stratifications | Slightly erosional surfaces covered by shells accumulations | *Crassostrea gryphoides* buildups | Planktonic foraminifera bryozoans, coralline algae, *Clypeaster* sea-urchins and *Crassostrea gryphoides* | **Middle-ramp**. Calm open mesophotic environment dominated by heterozoan benthic associations sporadically impacted by storms (shell accumulations). |
| **Flat-Topped Coral Platform (Depositional Profile 2)** Enamorados Limestones, Hondo Mbr | | | | | | | |
| **Ip** (Fig. S2A, Supplemental material) | Coarse-grained siliciclastic-rich calcarenite with disseminated basement pebbles | 27% | Horizontal stratifications | Rounded to subrounded pebbles. Alternation with Bhy facies | *Gastrochaenolites* and *Clionia* burrows | Oysters, barnacles | **Shallow inner carbonate platform** environment, dominated by heterozoan benthic communities with episodic supplies of siliciclastics supplied by alluvial fans (Franseen et al. 1997; Thrana and Talbot 2006). |
| **Op** (Figs. S2B, S2C, Supplemental material) | Coarse-grained calcarenite with rhodoliths and disseminated siliciclastics and coral clasts | 5% | Horizontal stratifications | Basinward transition from rhodolith-rich calcarenites to *Tarbellastraea* and *Porites* dominated facies colonizing a flat surface. | *Tarbeallastraea* and *Porites* buildups, *Gastrochaenolites*, rhodoliths | *Clypeaster*, pectinids, domal and columnar *Tarbellastraea*, lamellar and branching *Porites* | **Outer-platform** environment moderately affected by terrigenous input (Bosence 1983; Vennin et al. 2004; Montaggioni and Braithwaite 2009; Saelen et al. 2016). Bioclastic material provided by the mechanical erosion of the platform edge. |
| **Pe** (Fig. S2D, Supplemental material) | Coarse-grained calcarenite with coral clasts | 5% | Upper part of prograding clinoforms (dip up to 10°) | – | Closely spaced frame supported *Porites* buildups with branches encrusted by coralline algae | Domal, columnar, and thick branching *Porites*, encrusting red algae, echinoderms, *Ostrea edulis*, gastropods, pectinids | **Platform edge**. High-energy environments permanently impacted by waves (Pomar 1996; Pomar and Ward 1999; Pomar et al. 2004, 2012; Reuter and Brachert 2007; Montaggioni and Braithwaite 2009; Palmer et al. 2010; Brandano et al. 2016; Martin-Garin and Montaggioni 2023). |

TABLE 1.—*Continued.*

| Facies Associations | Lithology | Siliciclastic Content | Geometry | Sedimentary Structures and Spatial Facies Distribution | Biogenic Structures | Biotic Content | Interpretations |
|---|---|---|---|---|---|---|---|
| **Us** (Fig. S2E, F, Supplemental material) | Medium- to fine-grained calcarenite | < 5% | Middle part of prograding clinoforms (dip up to 15°) | _ | Closely spaced *Porites* buildups with branches encrusted by coralline algae | Thick robust branching *Porites*, echinoderms, *Ostrea edulis*, pectinids | **Upper-slope**. High-energy wave resitant environment indicated by the dominance of thick branching robust coral forms (Montaggioni and Braithwaite 2009, Pomar et al. 2004). |
| **Ls** (Fig. S2G, H, Supplemental material) | Fine-grained calcarenite | < 5% | Distal continuation of clinoforms (dip up to 5°) | Lenticular coral beds several tens of meters in lateral extent. Reworked *Porites* branches, reworked *Ostrea edulis*, and clasts of coralline algae. Basinward transition from facies Us | Coral carpets of thin branching *Porites* | Thin branching *Porites*, rare *Acanthastraea, Ostrea edulis*, echinoderm clasts, branching and columnar coralline algae | **Lower-slope**. Moderate-energy environment sporadically impacted by storms (Vennin et al. 2004; Reuter and Brachert 2007). |
| **Ts** (Fig. S2I–M, Supplemental material) | Fine-grained calcarenite | < 5% | Planar to low angle stratifications | Basinward transition from facies Ls | *Crassostrea gryphoides* buildups, diffuse bioturbation | *Crassostrea gryphoides*, fragile branching coralline algae, echinoderm clasts, planktonic foraminifera | **Toeslope**. Calm distal environment below the storm wave base in a normal marine setting with *Crassostrea* buildups on toe of slope (Bosence 1983; Jimenez et al. 1991; Perrin et al. 1995; Puga-Bernabeu et al. 2007; Ruchonnet and Kindler 2010). |
| ***Los Cautivos*** | | | | | | | |
| **Narrow Siliciclastic-Rich Coral Platform (Depositional Profile 3)** | | | | | | | |
| Lower and Upper Ruzafas Limestones | | | | | | | |
| **Inp** (Fig. S3A, B, Supplemental material) | Unsorted and clast or matrix support conglomerates. Coarse-grained bioclastic calcarenite with siliciclastic grains | 78% | Planer stratifications | Basinward pinch-out of conglomeratic beds | _ | Reworked massive *Tarbellastraea* and *Porites*, clasts of bivalves and echinoderms | **Inner narrow platform**. Basement pebbles and gravels provided by alluvial-fans (Postma 1990b) and intercalated in calcarenites provided by the mechanical erosion of the reef. |
| **Npe** (Fig. S3C, D, Supplemental material) | Coarse-grained calcarenite | 10% | Landward low-angle oblique stratifications | Landward transition to Inp facies. Proximal to distal transition from encrusting to massive domal and to thick-branching dominated coral forms | Frame supported coral buildups, *Gastrochaenolites* burrows, corals encrusted by coralline algae | Lamellar encrusting, massive domal, and thick branching *Tarbellastraea* and *Porites*, coralline algae, pectinids | **Narrow platform-edge**. Frame-supported and wave-resistant agitated depositional environment above the fair-weather wave base and impacted by sporadic siliciclastic inputs (Pomar and Ward 1999; Montaggioni and Braithwaite 2009) dominated by photozoan benthic associations. Relief formed by coral buildups (landward migration). |

TABLE 1.—*Continued.*

| Facies Associations | Lithology | Siliciclastic Content | Geometry | Sedimentary Structures and Spatial Facies Distribution | Biogenic Structures | Biotic Content | Interpretations |
|---|---|---|---|---|---|---|---|
| **Enp** (Fig. S3E, Supplemental material) | Siliciclastic-rich, medium to fine-grained calcarenite | 8% | Basinward slightly inclined beds (dip up to 10°) | _ | Diffuse bioturbation | Bryozoan, coralline algae, echinoderms, bivalves, planktonic foraminifera | **External narrow platform**. Calm distal mesophotic environment below the storm-wave base and dominated by heterozoan benthic associations (Johnson et al. 2005; Braga et al. 2006). |
| **Siliciclastics** | | | | | | | |
| ***Los Cautivos*** | | | | | | | |
| **Gilbert Delta** | | | | | | | |
| Lower and Upper Sandstones, Los Cautivos Conglomerates | | | | | | | |
| **Mbg** (Fig. S4A, Supplemental material) | Polygenic conglomerates (basement, Mesozoic sedimentary cover) and sandstones | | Meter-thick bodies pinching out basinward onto the upper part of the Gilbert delta foresets | Low angle internal progradation. Sharp vertical transition from clast-supported conglomerates with basinward pebble imbrications to sandstones | _ | Bilvalve clasts, vegetal remains | **Mouth-bars**. Hyperpycnal flows with pebbles transported as a traction carpet (Postma et al. 1988). Sandy deposits due to the settling of material out of suspension when the sediment-laden river flow mixed with marine waters (Orton and Reading 1993; Mutti et al. 2000). |
| **Uf** (Fig. S4B–D, Supplemental material) | Conglomerates and coarse-grained sandstones | | Inclined beds with dip between 20 and 30° | Alternation of: – polygenic matrix or clast-supported conglomerates with slightly erosional basal surfaces, internal progradational geometries truncated by sharp surfaces – coarse sandstones with layers of aligned isolated pebbles and cobbles, beds prograding upslope on a concave-upward truncation surface with upslope decrease of dip angles | *Ophiomorpha* burrows, *Gastrochaenolites* borings, | *Ostrea edulis,* Barnacles | **Upper-foresets**. Cohesive or non-cohesive debris-flow deposits truncated by slide surfaces formed by subaqueous landslides. Inertia-dominated homopycnal flow deposits and avalanching deposits (layers of aligned pebbles or isolated cobbles) (Nemec 1990; Orton and Reading 1993). Backsets due to hydraulic-jumps of hyperconcentrated underflows during storm or flood events in chute depressions (Massari and Parea 1990; Nemec 1990; Breda et al. 2007). |
| **Lf** (Fig. S4E–G, Supplemental material) | Coarse-grained sandstones and conglomerate layers | | Inclined beds with dip between 5 and 15° | Normal vertical grading in conglomerates overlain by coarse sandstones and gravels with planar laminae and sometimes by medium sands with scarce current ripples | Undetermined vertical burrows | Disseminated or small lenticular buildups of barnacles and *Ostrea edulis* | **Lower-foresets**. High-density turbidites (Breda et al. 2007; Ghinassi 2007; McConnico and Bassett 2007; Winsemann et al. 2007, 2009). |

TABLE 1.—*Continued.*

| Facies Associations | Lithology | Siliciclastic Content | Geometry | Sedimentary Structures and Spatial Facies Distribution | Biogenic Structures | Biotic Content | Interpretations |
|---|---|---|---|---|---|---|---|
| **Bs** | Fine grained sandstones and mudstones | | Distal continuation of foresets, dip about 5° | Alternation of 5- to 15-cm-thick beds of fine-grained sandstone with planar laminae, currents ripples, and 1–5-cm-thick mudstone layers | Undetermined vertical burrows | Undifferentiated bivalve clasts, planktonic foraminifera | **Bottomsets**. Middle to low-density turbidites (Stow and Shanmugam 1980; Nemec 1990; Breda et al. 2007; Backert et al. 2010). |
| | | | | **Shoal-Water Delta** Lower and Upper Sandstones | | | |
| **Mbw** (Fig. S4H, Supplemental material) | Conglomerates and sandstones | | Meter-thick bodies pinching out basinward | Low-angle internal progradation, landward imbrication of flat pebbles on top | _ | Bilvalve clasts, vegetal remains | **Mouth-bars reworked by waves**. Prograding mouthbar with beach deposits on top (Massari and Parea 1990). |
| **Df** (Fig. S4I–K, Supplemental material) | Medium- to fine-grained sandstones and unsorted conglomerate beds | | Planar stratification without break in depositional slope | Planar laminae and bidirectional symmetrical wave ripples in sandstones. Unsorted conglomeratic beds, with a lateral extension of several tens of meters and erosional bases. Lateral transition with mouth-bars over short distances (about 10 to 20 m) | *Ophiomorpha* burrows in sandstones | | **Delta-front (foreshore to shoreface)**. Collapse of a part of in-suspension material due to the mixing of sediment-laden river flow with marine waters (Mutti et al. 2000; Orton and Reading 1993). Deposits impacted by waves with intercalations of scour-filling hyperpycnal-flow deposits during surge or storm events (Mutti et al. 2000, 2003). |
| **Uo** (Fig. S4L, Supplemental material) | Heterolithic units with alternations of mudstones and 5- to 20-cm-thick medium-grained sandstone beds | | Planar stratification without break in depositional slope | Sandstones with a sharp faintly erosional basal surface, crude normal grading, and undulating HCS-like laminae draped by current ripples. Lateral transition with shoreface deposits | Undetermined vertical burrows | Planktonic foraminifera, echinoderm clasts, bivalves clasts | **Upper-offshore**. "Flood-generated delta front sandstone lobes" of Mutti et al. (2003) produced by hyperpycnal currents passing over mouth-bars. Distal part of turbulent density-flow deposits (low-density hyperpycnal flows) (Mutti et al. 2003). Settling of the fine-grained material transported basinward over large distances by buoyant hypopycnal flows (mudstones) (Orton and Reading 1993). |

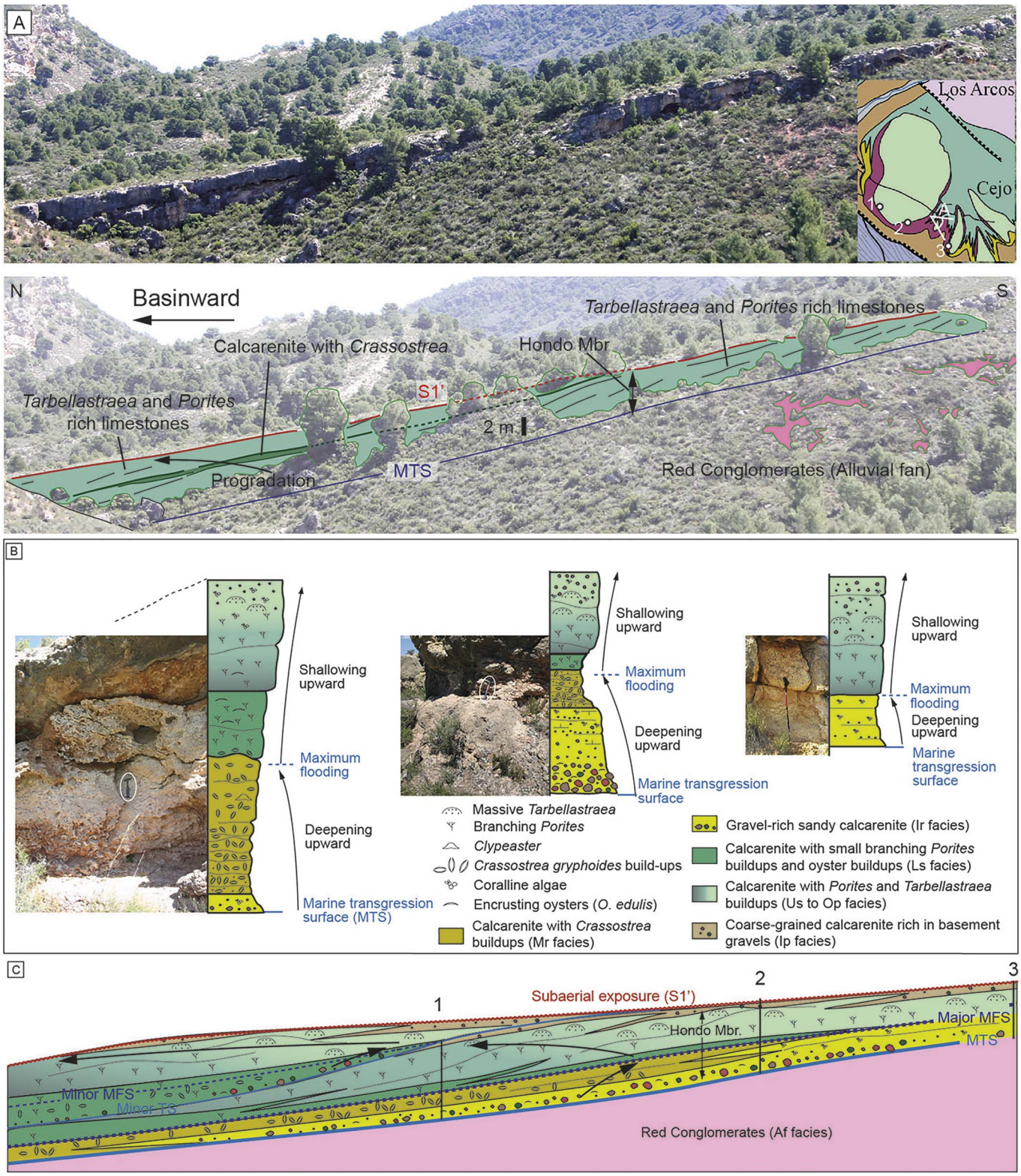


FIG. 5.—Geometries and sedimentological features of the Hondo Mbr in the Los Arcos area. **A)** Flat northwestward-prograding geometry covering a marine transgression surface in the area of the section 3 (Fig. 4A). **B)** Vertical stacking of facies in sections 1, 2, and 3. The thickness of the units and outer-platform facies increases northwestward. **C)** Prograding architecture of facies in the Hondo Mbr between sections 1, 2, and 3.

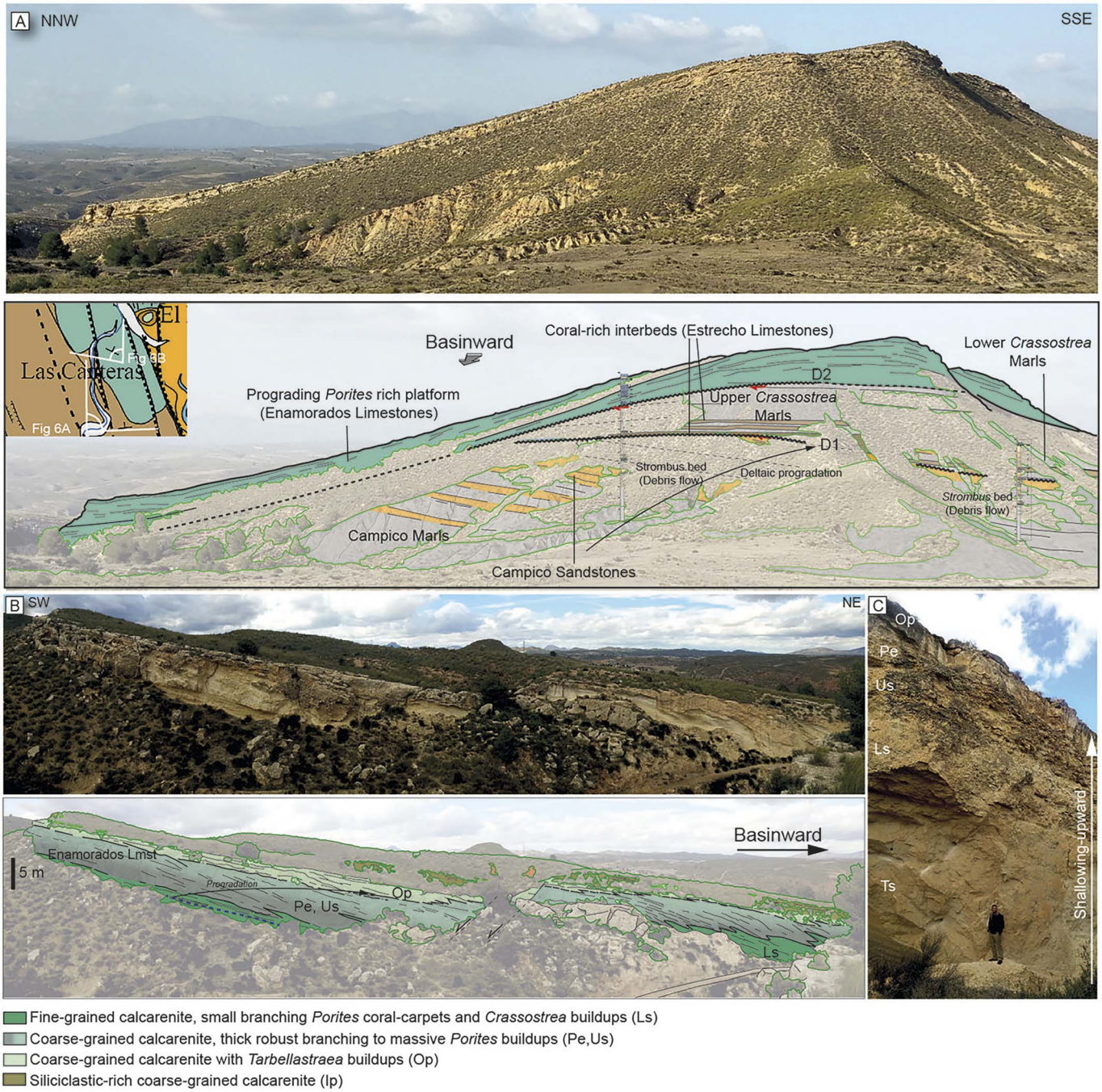


FIG. 6.—Geometries of the Enamorados Limestones Mbr in the Las Canteras area. **A)** Panorama of the western side of the Las Canteras outcrop. The prograding Enamorados Limestones Mbr covers the D2 angular unconformity. **B)** Panorama of the northern side of the Las Canteras valley showing the prograding geometry of the Enamorados Limestones with the transition from outer-platform to lower-slope facies along sigmoidal units. **C)** Vertical shallowing-upward evolution of facies in a sigmoidal unit. Fine-grained calcarenites of toeslope environment (Ts) are overlain by coral carpets (Ls) and then by thick branching and massive *Porites* (Us). The top of sigmoidal units consists of massive *Tarbellastraea* and *Porites* (Pe) covered by coarse-grained calcarenites (Op).

supported, polygenic conglomerates belonging to the Los Cautivos Fm (Bd facies, Table 1, Fig. S5E).

Interpretations: In the Coroneles Conglomerates, channelized conglomerates with crude oblique stratifications and sandstone sheets intercalated in red silty shales with paleosoils of the Mf facies are interpreted as braided alluvial-fan deposits with stream channels, sheetfloods, and alluvial-plain deposits, respectively (Fl and P facies of Miall 2006, Table 1). Ir facies correspond to an inner-ramp environment impacted by debris flows, and the coarse-grained matrix indicates an environment impacted by wave action above the storm-wave base (Table 1). This facies grades distally to *Heterostegina* shoal facies in the distal part of the inner ramp. Grainstone texture and grain size of this calcarenite indicate an agitated environment above the fair-weather wave base (Burchette and Wright 1992). The inner-ramp environment was dominated by heterozoan communities, and only small and disseminated *Porites* buildups are present. The absence of phototrophic organisms and the fine-grained

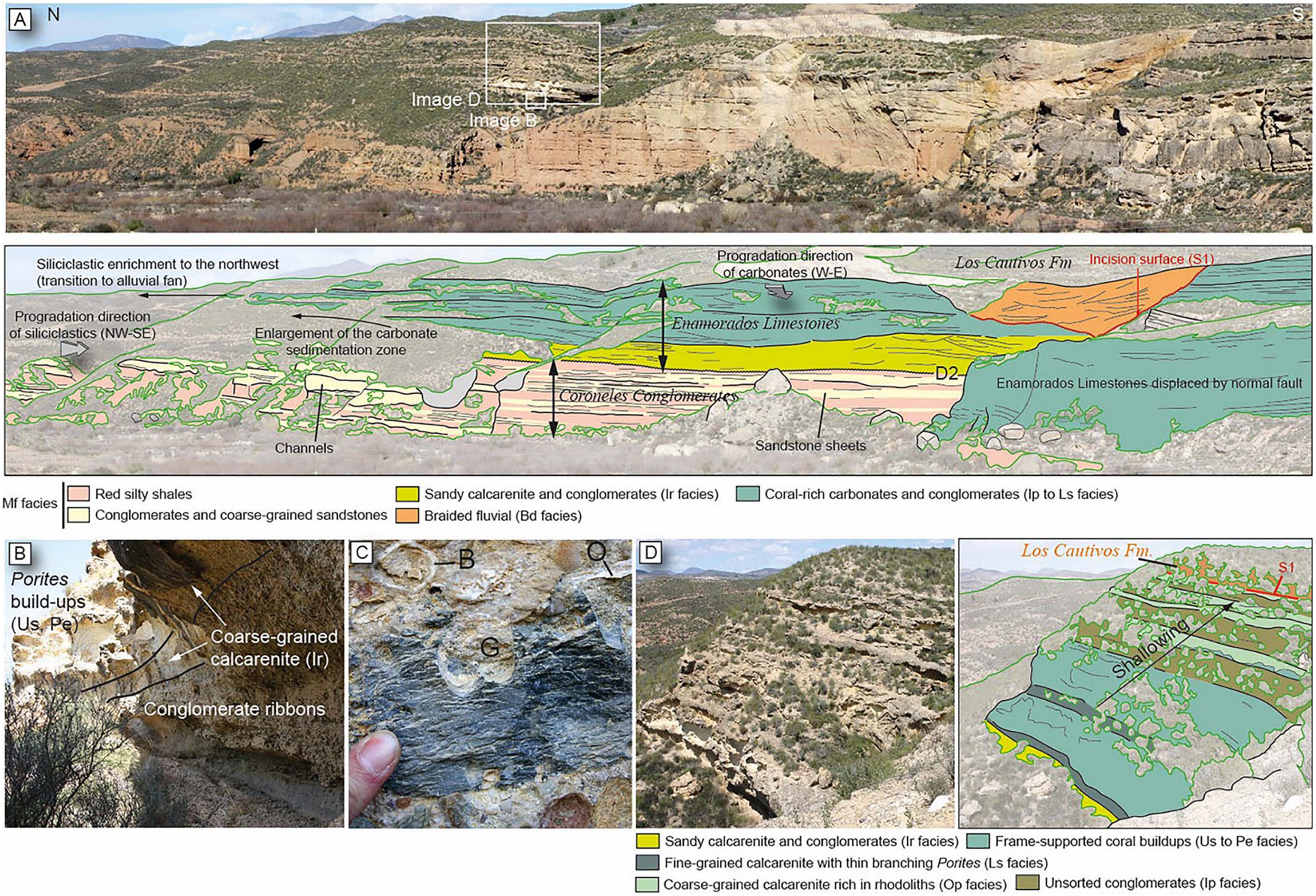


FIG. 7.—Geometries and sedimentological features of the Enamorados Limestones Mbr in the Los Cautivos area. **A)** Panorama of the Los Cautivos outcrop on the eastern side of the Guadalentine river. **B)** Early deposits at the base of the Enamorados Limestones characterized by inner-ramp facies (Ir). **C)** *Gastrochaenolites* borings in a basement pebble encrusted by an oyster (O). B, barnacle. **D)** Close-up view of the Enamorados Limestones shallowing upward evolution and their internal facies succession.

deposits of the Mr facies suggest that this facies was deposited in a calm, open mesophotic environment. The shell accumulations above erosional surfaces are interpreted as storm deposits in a middle-ramp environment, located above the storm-wave base. The Ip facies is dominated by heterozoan communities and was impacted by episodic supplies of basement-derived siliciclastics. These siliciclastic inputs and the coarse-grained matrix suggest an inner-platform environment close to alluvial systems, above the storm-wave base (Franseen et al. 1997; Thrana and Talbot 2006). In the Op facies, the local occurrence of large rhodoliths, and *Tarbellastraea* buildups, and the dominance of clasts mainly derived from mechanical erosion of coral buildups are consistent with an agitated outer-platform environment moderately affected by terrigenous input (Bosence 1983; Vennin et al. 2004; Montaggioni and Braithwaite 2009; Sælen et al. 2016). Thick branching and domal *Porites* with coarse-grained calcarenite of the Pe facies developed in a high-energy environment permanently impacted by waves at the platform edge (Pomar 1996; Pomar and Ward 1999; Pomar et al. 2004, 2012; Reuter and Brachert 2007; Montaggioni and Braithwaite 2009; Palmer et al. 2010; Brandano et al. 2016; Martin-Garin and Montaggioni 2023). The Us facies is made of frame-supported and closely spaced thick robust branching *Porites* adapted to environments with high fair-weather wave energy (Montaggioni and Braithwaite 2009; Pomar et al. 2004). It is interpreted as an upper-slope environment above the storm-wave base. In the Ls facies, the benthic fauna is dominated by thin branching *Porites* and rare *Acanthastraea* embedded in a fine grained calcarenite. The slender morphology of branching *Porites* and the alternation with fine-grained carbonates suggest a relatively low and intermittent hydrodynamic conditions above the storm-wave base in the lower slope (Reuter and Brachert 2007), which is consistent with the local occurrence of reworked *Porites* branches and reworked *Ostrea edulis*. The Ts environment is made of a fine-grained calcarenite with planktonic foraminifers, branching coralline algae, and small *Crassostrea gryphoides* buildups. In the Tortonian of the Betics, and unlike modern specimens living in brackish environments, *Crassostrea gryphoides* grew on soft substrates below the storm-wave base in a basinal setting under normal marine conditions (Jimenez et al. 1991). All the features of this Ts facies suggest a calm distal toeslope environment below the storm-wave base (Bosence 1983; Perrin et al. 1995; Puga-Bernabeu et al. 2007; Ruchonnet and Kindler 2010).

The Af facies of the Red Conglomerates is characterized by non-channelized, unsorted, clast-supported or matrix-supported continental conglomerates made of basement-derived material. These deposits are interpreted as deposits of a debris-flow-dominated alluvial-fan provided by neighboring basin margins (Gmm facies of Miall 2006). Filling the incisions on top of the Enamorados Limestones in Los Cautivos, the conglomeratic Bd facies with pebble imbrications, and trough cross-bedding implies a high-energy steady flow. The sedimentary characteristics of the Bd facies are consistent with braided-river deposits (Gh, Gt facies of Miall 2006).

**Lower and Upper Ruzafas Limestones Mbrs.—**Along the northern side of the Guadalentine valley in the Los Cautivos area (Fig. 8, location in Fig. 1D), Messinian Lower and Upper Ruzafas Limestones mbrs are intercalated with conglomerates and sandstones of the Los Cautivos Fm (Fig. 2). The Lower and Upper Ruzafas Limestones mbrs have similar internal stratigraphical and facies architectures, but due to their better outcrop conditions only the Upper Ruzafas Limestones are detailed here (Fig. 8). The Upper Ruzafas Limestones are intercalated between two siliciclastic units prograding to the east: the Upper Sandstones and Los Cautivos Conglomerates mbrs (Fig. 8). The Upper Sandstones Mbr consists of exotic polygenic sandstones and conglomerates (Wrobel and Michalzik 1999; Carpentier et al. 2020). The lower part of this member is characterized by an oblique progradation and the basinward lateral transition from: 1) polygenic conglomerates pinching basinward with low-angle internal progradations (Mbg facies, Table 1, Fig. S4A), 2) polygenic matrix or clast-supported conglomerates with slightly erosional basal surfaces, internal progradational geometries with dip between 20 and 30°, coarse-grained sandstones with layers of aligned isolated pebbles and cobbles, and locally oblique stratification prograding upslope over a concave-upward truncation surface with an upslope decrease of dip angles (Uf facies, Table 1, Fig. S4B–E), 3) coarse-grained sandstones and conglomerate layers with dip between 5 and 15°, normal vertical grading in conglomerates overlain by coarse sandstones and gravels with planar laminae and sometimes by medium sands with scarce current ripples. The fauna consists of barnacles and *Ostrea edulis* disseminated or forming small lenticular buildups (Lf, facies, Table 1, Fig. S4E–G), and 4) alternations of 5–15-cm-thick and 5° dipping beds of fine-grained sandstones with beds characterized by planar laminae, currents ripples, and 1–5-cm-thick mudstone layers containing planktonic foraminifera (Bs facies, Table 1).

A sigmoid progradation is observed in the upper part of the Upper Sandstones (Fig. 8). It should be noted that the sedimentary slope becomes gentler in the upper part of the Upper Sandstone Mbr, where the depositional profile tends to flatten out (Fig. 8). The basinward transition of facies is characterized by: 1) meter-thick conglomerates and sandstones with low-angle internal progradation and landward imbrication of flat pebbles on top (Mbw facies, Table1, Fig. S4H), 2) medium- to fine-grained sandstones with symmetrical wave ripples, *Ophiomorpha* burrows, and unsorted conglomerate beds with a lateral extension of several tens of meters (Df facies, Table 1, Fig. S4I–K), and 3) heterolithic alternations of mudstones and 5–20-cm-thick medium-grained sandstone beds with crude normal grading, and undulating HCS-like laminae draped by current ripples (Uo facies, Table 1, Fig. S4L). A first *Porites* buildup is embedded within the Lower Sandstones (Fig. 8). Colonies of *Porites* appear at the top of conglomeratic submarine deposits of the Mbw facies. This colonization by photozoan communities coincides with the maximum landward enlargement of this first carbonate episode (Fig. 8). The uppermost deposits of the Upper Sandstones Mbr are impacted by a synsedimentary sliding surface (Figs. 8, 9A).

The Upper Ruzafas Limestones are subdivided into two main carbonate units (1 and 2 in Fig. 9A), separated by conglomeratic deposits that pinch out basinward. Both carbonate units show a gradual enlargement and shoreward-sloping depositional geometries (Fig. 9A, D). They indicate a progressive landward migration of carbonates. The Upper Ruzafas Limestones overlie clast-supported conglomeratic deposits of the Mbw facies. They consist of frame-supported and poorly diversified buildups made of domal and branching *Tarbellastraea* and *Porites* with rare platy to dish-shaped *Porites* (Vennin et al. 2004) in a coarse-grained calcarenite (Npe facies, Table 1, Fig. 9B, C, Fig. S3D). They constitute the thickest part of the Upper Ruzafas Limestones Mbr. In the proximal NW area, the siliciclastic content increases while domal and branching corals are replaced by lamellar and encrusting forms (Fig. S3C). These deposits alternate with coarse-grained and siliciclastic-rich calcarenites containing reworked *Tarballastraea* and *Porites* (Inp facies, Table 1, Fig. 9A, Fig. S3A, B). Basinward, a truncation surface crosscuts carbonate unit 1 and the top of the Upper Sandstone Mbr (Figs. 8A, 10A). Eastward, the surface is sharp and crosscuts underlying sediments at a low angle (Fig. 10A). It is covered by conglomerates mixed with coral boulders probably reworked from unit 1 (Fig. 10A, B). The conglomeratic infill above the truncation surface contains locally large 1–2-m-high landward-prograding oblique stratification (Fig. 10A). Upslope, conglomerates are gradually replaced by carbonates rich in basement pebbles and containing coral buildups dominated by *Porites* (Fig. 10C). Conglomerates are covered by

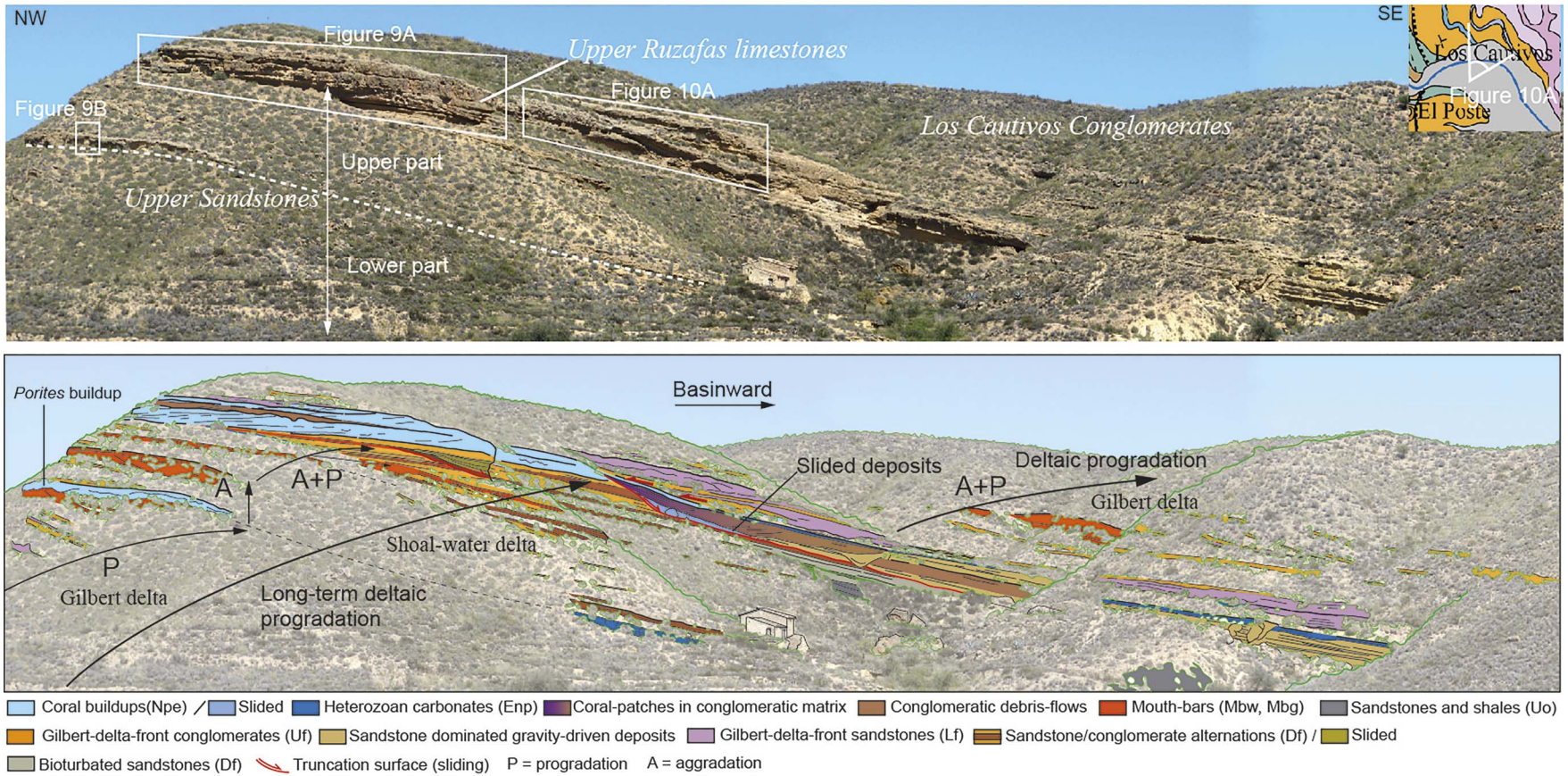


FIG. 8.—Geometries, sedimentological features, and facies succession of the Upper Ruzafas Limestones Mbr in Los Cautivos.

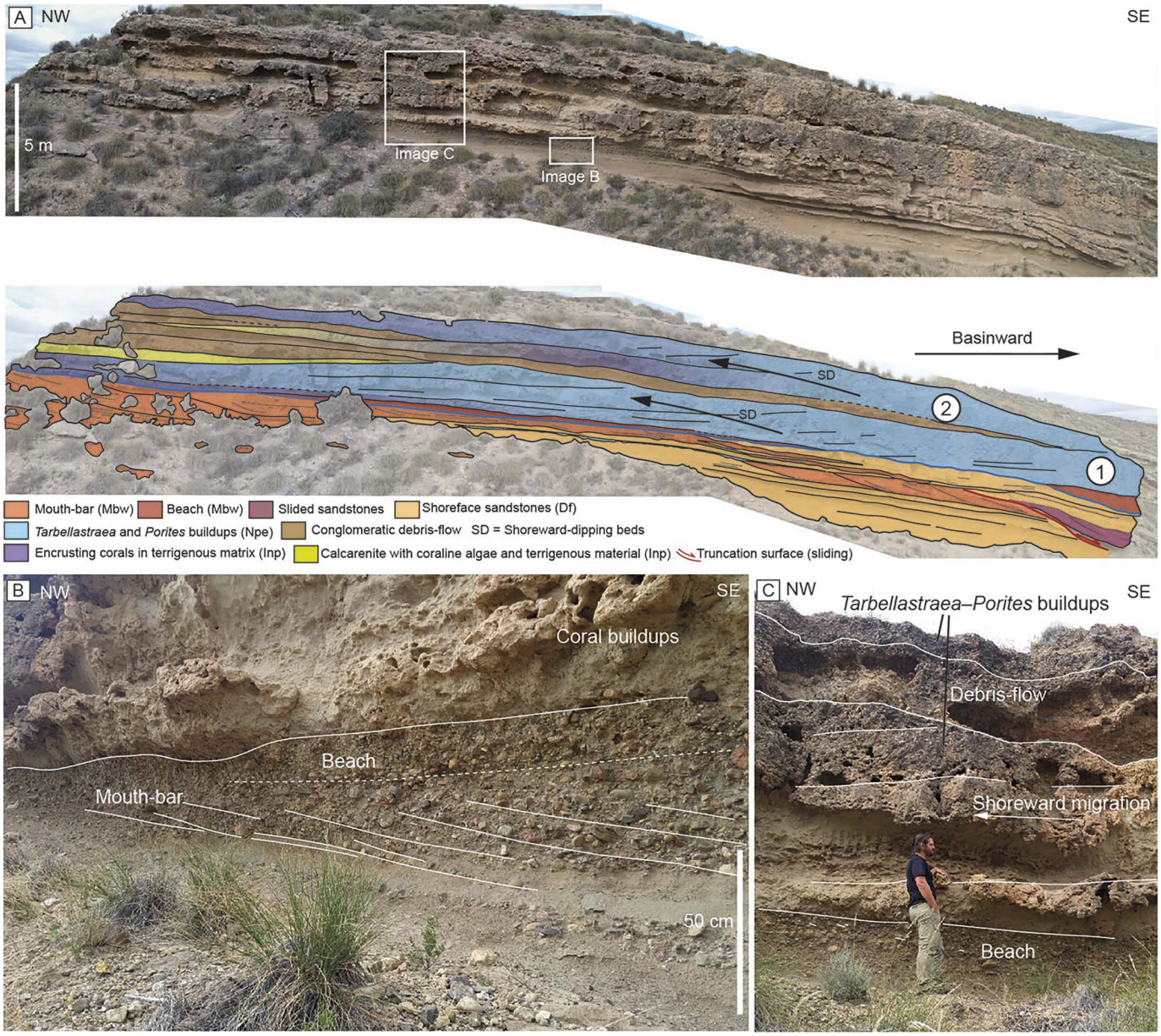


FIG. 9.—Close-up view of the Upper Ruzafas Limestones Mbr in the northwestern part of the outcrop. **A)** Interpretive panorama. The shoal-water delta is characterized by a flat geometry with a lateral transition from conglomeratic and sandy mouth bars to foreshore and shoreface sandstones. The reefs show landward retrogradation and a transition to encrusting forms in the proximal direction. Note the intercalation of debris flows between reef units 1 and 2. **B)** Detail of the vertical transition from shoal-water deposits with beach deposits on top of a conglomeratic mouth bar to coral buildups. This transition is accompanied by a significant decrease in siliciclastic content. **C)** Close-up view of the Upper Ruzafas Mbr showing the intercalation of conglomeratic debris-flow deposits between retrograding reefal units 1 and 2.

carbonate unit 2 (Fig. 10A), which is characterized by the lack of significant basinward progradation and also by a dominant landward migration as for unit 1. Unit 2 grades laterally basinward into *Porites*-dominated buildups and bioturbated sand-rich carbonates over a short distance of about 10 m (Fig. 10A). These deposits contain planktonic foraminifera and a heterozoan benthic association dominated by ectoprocts (bryozoan), echinoderms, bivalves, and scarce coralline algae (Enp facies, Table 1, Fig. S3E). Unit 2 is overlain by prograding sandstones and conglomerates of the Los Cautivos Conglomerates Mbr (Fig. 8). They show the same facies organization as the Upper Sandstones conglomerates.

Interpretations: The Mbg, Uf, Lf, and Bs facies of the lower part of the Upper Sandstones Mbr are interpreted as Gilbert-delta sandstones and conglomerates showing a lateral transition between mouth bars, foresets with backsets, and bottomsets facies (Table 1). Topset deposits are not visible. The upper part of the Upper Sandstones with a sigmoid progradation geometry corresponds to shoal-water delta deposits impacted by waves without a marked slope break (Fig. 8A, Table 1). In a basinward direction, flat conglomeratic mouth bars reworked by waves grade laterally to delta-front sandstones with scour-filling conglomerates and *Ophiomorpha* burrows, and finally to upper offshore heterolithic facies (Mbw, Df, Uo facies).

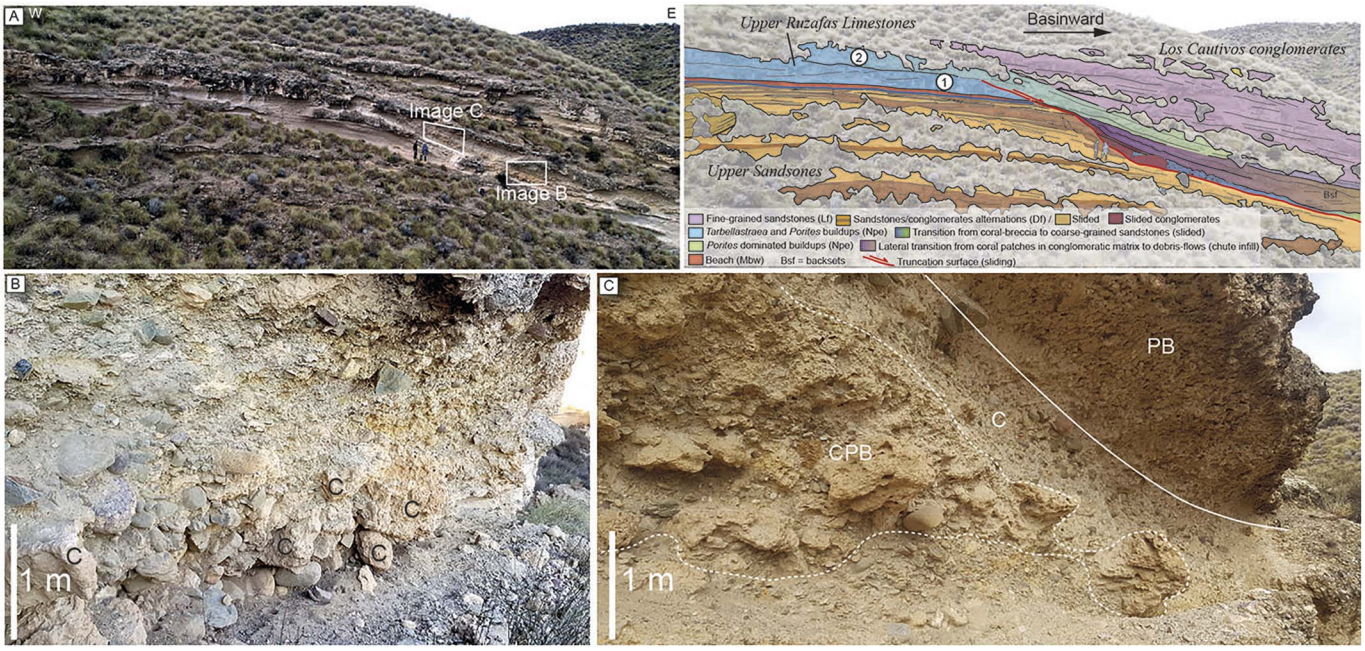


FIG. 10.—Close-up view of the Upper Ruzafas Limestones Mbr in the south-eastern part of the Los Cautivos outcrop. **A)** Interpretive panorama of the lateral transition from platform carbonates to slided and chute-fill deposits with backsets. The landslide and the deposition of coarse-grained debris flows occurred before the recolonization of the platform by corals of the reefal unit 2. **B)** Reworked coral boulders (C) mixed with conglomerates above the slide surface. **C)** *In situ* coral buildups (CPB) intercalated with a pebble-rich matrix (C) in the last stages of the chute fill. They are covered by *Porites*-dominated buildups (PB).

Coarse-grained deposits, characterized by unsorted conglomerates and reworked corals of the Inp facies, indicate a proximal inner narrow platform shallow-marine environment that was impacted by siliciclastic inputs provided by alluvial fans (Postma 1990b). These deposits are intercalated in calcarenites resulting from the mechanical erosion of the reef. In the Npe facies, the landward-oriented oblique stratification in coral buildups indicates that they formed a relief above the seafloor. Compared to Quaternary coral reefs, the prevalence of massive domal morphologies, along with robust branching forms and coarse-grained calcarenite, suggests relatively high hydrodynamic conditions above the fair-weather wave base on a narrow platform edge (Montaggioni and Braithwaite 2009; Perrin et al. 1995; Reuter and Brachert 2007; Brandano et al. 2016). In the Enp facies, coral buildups are replaced by bioturbated medium- to fine-grained calcarenites with terrigenous grains and planktonic foraminifers. This facies indicates a calm distal mesophotic environment dominated by heterozoan benthic associations below the storm-wave base (Johnson et al. 2005; Braga et al. 2006).

The low angle of the truncation surface, which crosscuts the first reef unit, is overlain by conglomerates and reworked coral boulders. It suggests that the surface was generated by a large subaqueous landslide. The landward prograding stratification in the conglomerates is interpreted as backsets in chute-fill deposits. They are coeval with debris-flow deposits observed between carbonate units 1 and 2 in the western part of the outcrop (Fig. 9A). The landward transition from conglomerates to coral buildups dominated by *Porites* (Fig. 10C) marks the initial coral-recolonization phase after the landslide, likely facilitated by the presence of a hard substrate formed by conglomeratic pebbles.

### *Depositional Models*

For carbonate deposits, as explained above, lateral transitions of carbonate facies and variations of depositional profiles along proximal–distal transects have been observed in outcrops of the Lorca Basin. On the basis on these observations, three depositional models are proposed: 1) homoclinal heterozoan ramp, 2) flat-topped coral platform, and 3) narrow siliciclastic-rich coral platform (Fig. 11).

**Depositional Model 1: Homoclinal Heterozoan Ramp.—**This first depositional model corresponds to the lower parts of the Enamorados Limestones and Hondo mbrs. Most proximal inner-ramp facies (Ir), rich in siliciclastics, contain an average siliciclastic content of 85% (Fig. 11D). In the distal part of the inner ramp, this Ir facies grades to coarse-grained shoal deposits rich in *Heterostegina* and disseminated rhodoliths. These inner-ramp deposits grade laterally basinward to middle-ramp facies (Mr facies), which are relatively rich in terrigenous silts (6%, Fig. 11D).

**Depositional Model 2: Flat-Topped Coral Platform.—**This second depositional model is proposed for deposits observed in the upper parts of the Enamorados Limestones and Hondo mbrs. The lateral distribution of facies is supported by observations along clinoforms in the Las Canteras outcrop for the Enamorados Limestones and in the Los Arcos area for the Hondo Mbr (Figs. 5, 6). The benthic communities are dominated by photozoan organisms. The coral buildups did not form any relief. The colonies formed coral-carpet beds organized in sigmoid rather than a true reefal architecture. These sigmoids with coral carpets constitute the platform edge at the margin of a flat-topped platform profile (Fig. 11B).

Inner-platform facies contain about 27% gravels, pebbles, and sand (Ip facies) (Fig. 11B). They pass laterally to open-platform facies (Op facies). The siliciclastic content decreases to 5% of the sediment volume. The upper part of clinoforms is represented by the platform-edge facies (Pe facies). It grades laterally basinward to upper-slope deposits (Us facies). The lower part of the slope is represented by the Ls facies, grading laterally basinward to toeslope deposits (Ts facies). The siliciclastics content never exceeds 4% from platform-edge to toeslope environments (Fig. 11D).

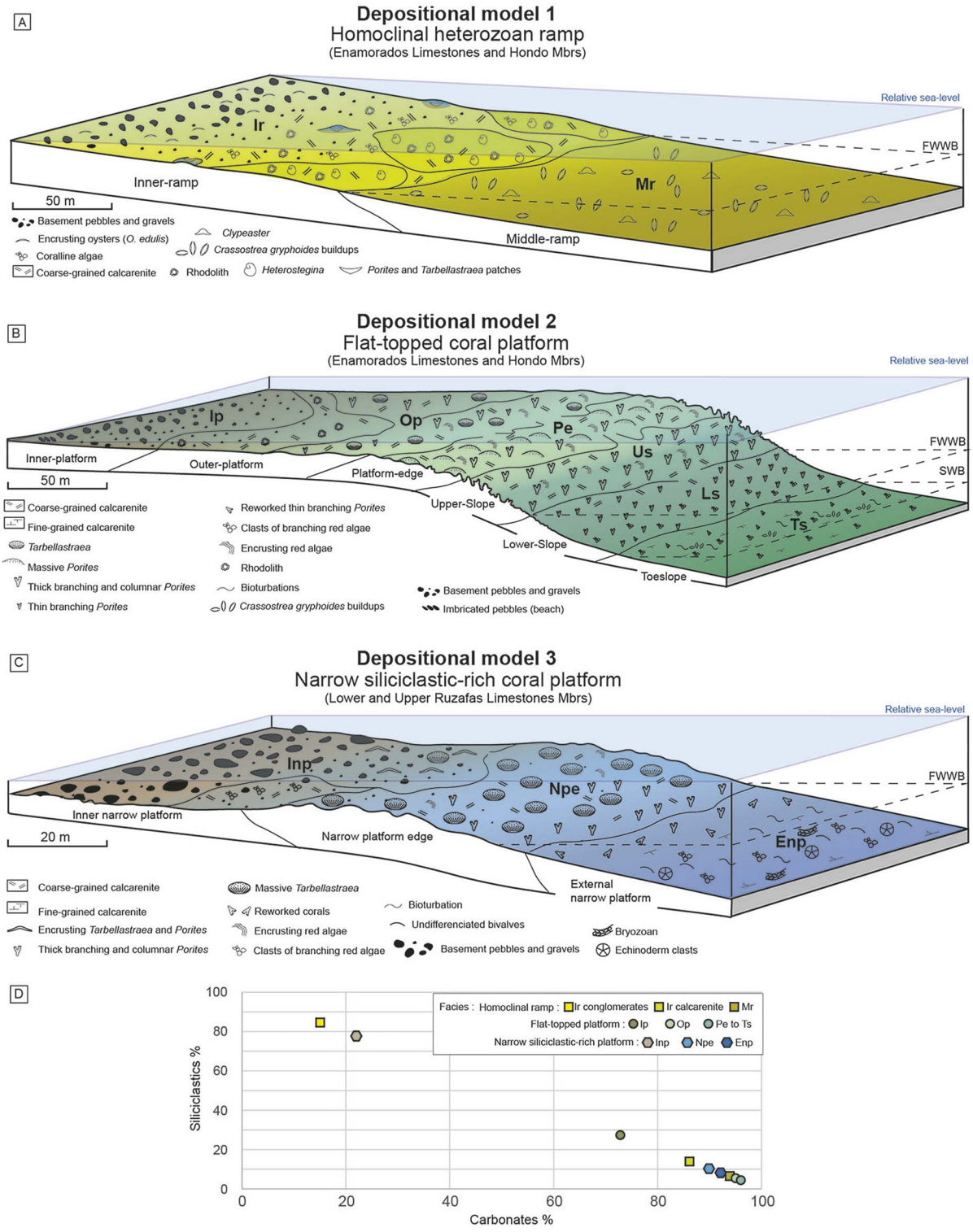


FIG. 11.—Depositional-environment models of the three types of carbonate profiles in the late Tortonian and early Messinian of the Lorca Basin and average siliciclastic contents of facies.

**Depositional Model 3: Narrow Siliciclastic-Rich Coral Platform.—** A narrow siliciclastic-rich coral platform is proposed for the Lower and Upper Ruzafas Limestones. This platform is intercalated in deltaic deposits and is only few tens of meters in lateral extent. The most proximal facies consist of unsorted clast-supported conglomerates or carbonate-matrix-supported conglomeratic sediments (Inp facies) (Fig. 11C). The gravels, pebbles, and sand-size siliciclastic grains constitute about 78% of the sediment volume (Fig. 11D). The platform edge encompassed frame-supported corals with a siliciclastic content of about 10% (Npe facies). The proportion of encrusting corals and

siliciclastics in the matrix increases landward. In contrast, the proportion of branching *Porites* increases slightly basinward, but the number of corals decreases rapidly in the external platform and the siliciclastic content decreases to 8% (Enp facies).

## DISCUSSION

### *Sequence Stratigraphic Framework of Carbonates and Benthic Communities*

**Enamorados Limestones and Hondo Mbrs (Las Canterras–Los Arcos).—**The sequence-stratigraphic framework and variations in the A/S ratio were interpreted on the basis of both geometries observed at outcrop scale (sigmoid or oblique progradations, forced regression, retrogradation) and the vertical stacking of facies. The depositional sequences of the Enamorados Limestones and Hondo mbrs exhibit similarities in the composition and stacking pattern geometry, and their benthic associations, albeit with some specificities.

Transgressive System Tract (TST): The earliest deposits of the Enamorados Limestones and Hondo mbrs correspond to a homoclinal heterozoan ramp (depositional model 1). They are transgressive and cover the D2 unconformity (Enamorados Limestones Mbr) or a marine transgression surface (Hondo Mbr) (Fig. 12A, D). A retrogradation of depositional environments, marked by the vertical transition from inner-ramp to middle-ramp environments, is accompanied by a vertical decrease in the amount and grain size of siliciclastic sediments in inner-ramp facies (Fig. 4B). During the transgression, heterozoan benthic associations with large oysters dominated in the middle-ramp environment and coralline algae, occurring either alone or associated with *Heterostegina*, were abundant in the proximal inner-ramp environment.

Highstand System Tract (HST): The transgressive-ramp geometry (depositional model 1) evolved into a prograding flat-topped platform geometry (depositional model 2) during the highstand (Fig. 12B). *Crassostrea gryphoides* patches provided a hard substrate for the installation of the first coral colonies (Vennin et al. 2004). The vertical stacking of carbonate deposits, up to a thickness of 30 m for the Enamorados Limestones, indicates that positive accommodation developed during carbonate sedimentation. The sigmoid progradation observed in Las Canteras and the general shallowing of depositional environments indicates that the A/S ratio was positive but the sedimentation rate exceeded accommodation. At the same time, shallow carbonate facies retrograded onto siliciclastic deposits in the proximal parts of the profile (Fig. 12B). This also suggests that accommodation was high enough to generate a retreat of siliciclastics but was compensated in real time by the high *in-situ* carbonate production. Both the Enamorados Limestones and the Hondo mbrs exhibit a similar overall sequence stratigraphic pattern. However, unlike the Enamorados Limestones, the early highstand phase in the Hondo Mbr was marked by a rapid decline to zero in the accommodation rate, as evidenced by the oblique progradation directly above the transgressive deposits (Fig. 12E).

Lowstand System Tract (LST): Base-level drop at the top of the Enamorados Limestones led to an exposure and incision of the southern basin margin (S1 surface), marking the first signs of basin restriction during the Messinian (Carpentier et al. 2020) (Fig. 12C). Accommodation became negative, and this exposure can be interpreted as a forced regression (Hunt and Tucker 1992; Plint and Nummedal 2000; Catuneanu et al. 2009). After the S1 surface, a renewal in accommodation led to the deposition of debris-flow-dominated alluvial-fan deposits of the Red Conglomerates in Los Arcos and Las Canteras. The subaerial exposure (S1′ surface) on top of the Hondo Mbr also suggests that accommodation became negative and base level dropped after carbonate deposition (Fig. 12C, F).

**Lower and Upper Ruzafas Limestones Mbrs (Los Cautivos).—**HST: During the early stages of the Lower and Upper Sandstones mbrs, the oblique progradation indicates that the accommodation was low or null, and no vertical stacking of sediment occurred on the delta top (Fig. 13A). Carbonates were absent, and benthic communities were dominated by heterotrophic filter-feeding organisms such as *Ostrea edulis* and barnacles. In the upper parts of Lower and Upper Sandstones mbrs, small *Porites* buildups appeared on mouth bars in front of the delta (Fig. 13B). In the Neogene deltaic deposits of Borneo, Wilson and Lokier (2002) proposed that coral buildups located on mouth bars in the delta front developed in a water depth less than 10 m. Likewise, within the nutrient-rich waters of the Gulf of California, monospecific *Porites* buildups are found at depths ranging from 5 to 10 m (Halfar et al. 2005, 2006). A similar shallow paleodepth can be inferred for the low-diversity assemblage of *Porites* buildups on mouth bars in the Lorca Basin. These small buildups, dominated by photozoan communities, developed only when accommodation became positive and aggradation occurred on the delta top. However, the sigmoid progradation in the upper part of the Upper Sandstones indicates that the sedimentation rate exceeded the accommodation. These periods of positive accommodation at the end of highstands coincide with the flattening of sedimentary profiles and the transition from Gilbert-delta to shoal-water-delta systems (Fig. 13B), preceding the installation of the Lower and Upper Ruzafas Limestones.

TST: The first constructions of the Lower and Upper Ruzafas Limestones were established on flat surfaces above beaches and delta-mouth bars (Fig. 13C). They show a landward migration of carbonate buildups indicated by shoreward-sloping depositional geometries. In contrast to the Lower Ruzafas Limestones, the Upper Ruzafas Limestones are organized in two carbonate units (1 and 2 in Figs. 9, 10). They are separated by a subaqueous landslide that temporarily interrupted carbonate sedimentation (Fig. 13D). Following this event, coral growth restarted, as illustrated by the development of constructions in a pebble-rich matrix. This suggests that the base level did not change between the two reef units and that carbonate production was only interrupted by the temporary input of coarse-grained siliciclastic material. The recolonization by corals terminated with the deposition of coral unit 2 (Fig. 13D). Similar alternations between carbonates and siliciclastics were described by Reuter and Brachert (2007) in the Tortonian of Crete, where massive colonies of *Tarbellastraea*, *Porites*, and *Acanthastraea* colonized the top of Gilbert-delta deposits. These authors proposed that massive colonies developed in a water depth of about 20 m. Garcia-Garcia et al. (2006) considered that buildups intercalated between Gilbert-delta deposits during flooding events in the Tortonian of the Tabernas Basin were deposited in only a few meters depth. These authors interpreted coral facies as early transgressive deposits and considered that the maximum water depth was reached during the deposition of overlying calcarenites rich in coralline algae. In the Lorca Basin, *Tarbellastraea* and *Porites* buildups are directly covered by prograding Gilbert-delta foresets. This suggests that the maximum water depth was reached here during the growth of coral colonies. Considering the vertical thickness of the overlying Gilbert-delta foresets, a water depth of at least 10 m can be estimated for the deposition of carbonates.

LST: The *Tarbellastraea* and *Porites* buildups of unit 2 were gradually covered by prograding Gilbert-delta deposits during a new highstand of the relative sea-level (Fig. 13E). This return to high siliciclastic input was associated with the reappearance of heterotrophic-dominated assemblages.

### *Paleogeographical Evolution*

Facies distribution and interpretations of depositional environments are the basis of new paleogeographical maps for the southwestern part of the Lorca Basin (Fig. 14). During the early stages of the Enamorados Limestones, an alluvial fan was backed onto the basin margin in the Los

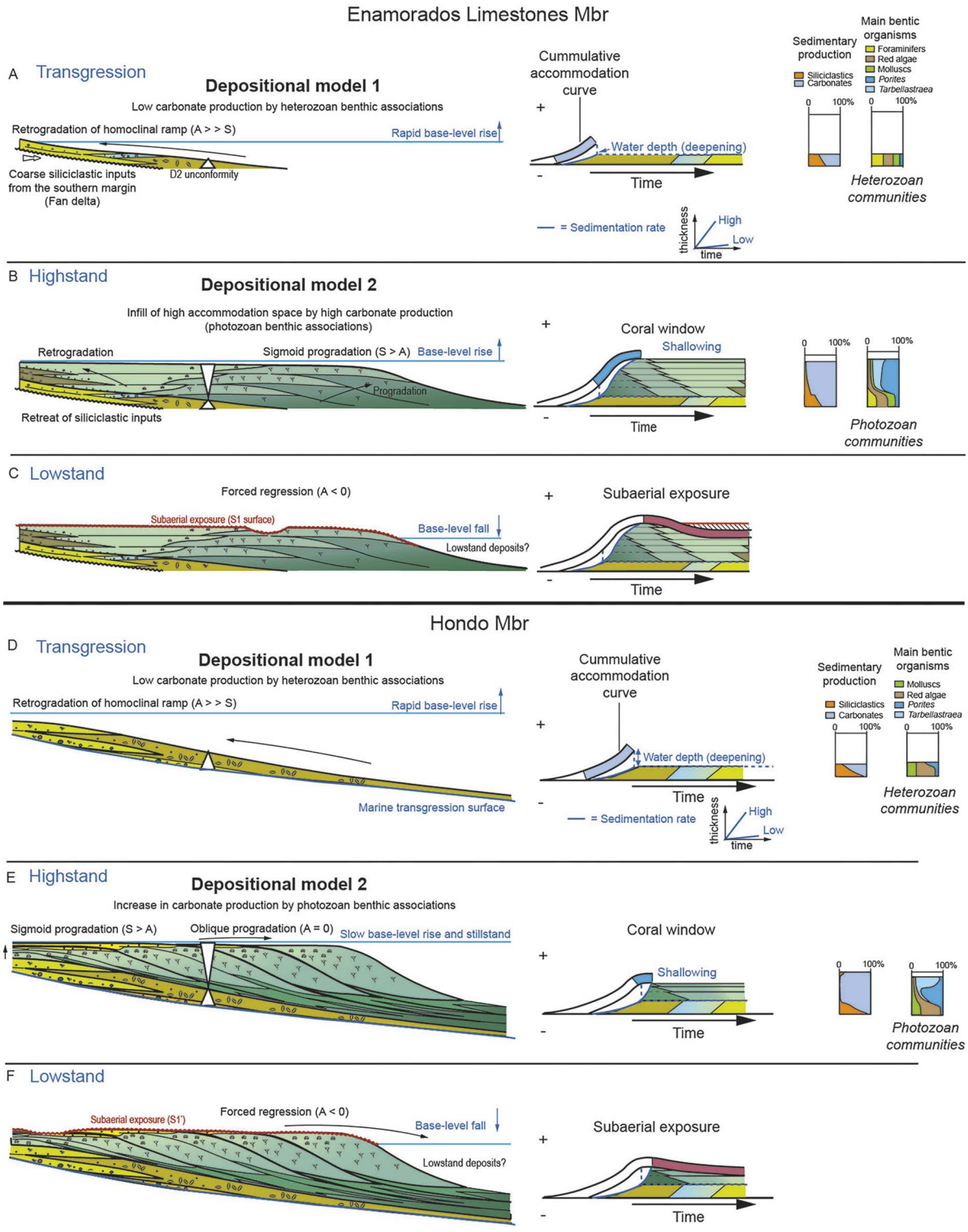


FIG. 12.—Relationships between geometries, accommodation, sedimentation rates, sediment types, and benthic communities for the Enamorados Limestones and Hondo mbrs.

Arcos area (Fig. 14A). It constituted a short alluvial system carrying only basement-derived clasts provided by the neighboring hinterland and acted as a local entry waypoint of coarse siliciclastic material. According to a basic calculation based on the surface area and the thickness of deposits, a volume of about 30 to 40 million $m^3$ of siliciclastics can be estimated. Northwest of Los Cautivos, a more mature and larger alluvial fan system arrived from the northwest and carried both local basement clasts and exotic material from Mesozoic cover of the external Betics (e.g., oolitic limestones) (Carpentier at al. 2020) (Fig. 14A). The volume of siliciclastic material transported by this mature system was probably at least three

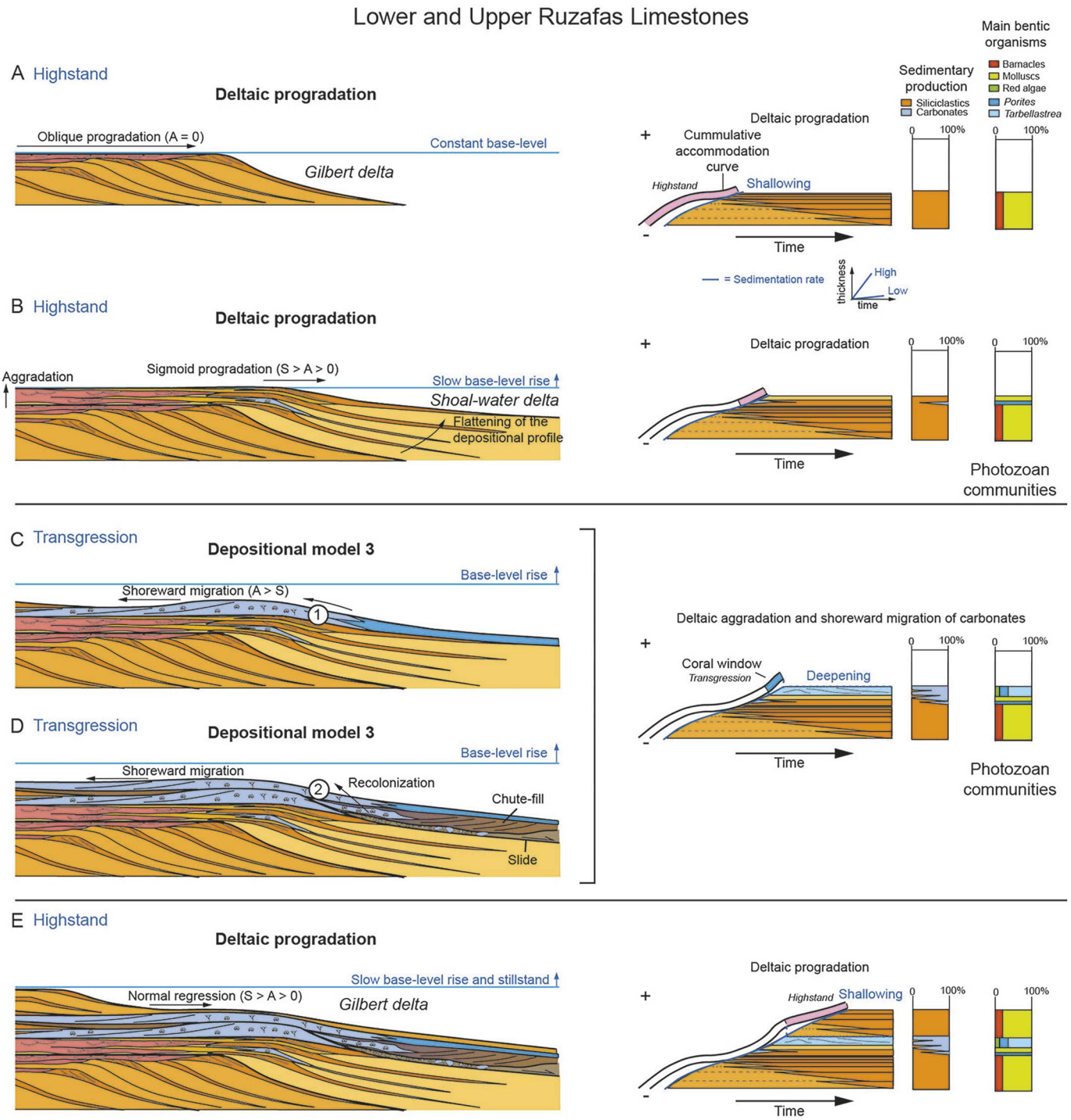


FIG. 13.—Relationships between geometries, accommodation, sedimentation rates, sedimentation types, and benthic communities for the Lower and Upper Ruzafas Limestones mbrs.

times more important than for the Los Arcos area (94 to 112 million $m^3$). A homoclinal carbonate ramp developed laterally and between entryway points of siliciclastics. This carbonate system gradually flooded alluvial fans that retreated landward (Fig. 14A).

During the late stages of the Enamorados Limestones, the homoclinal ramp was replaced by a prograding flat-topped coral platform (Fig. 14B). During the transgression and the highstand, carbonates gradually encroached on basin margins and covered part of the sources of siliciclastics. Siliciclastic sediments reentered the southern and northern parts of the basin only during the final stages of the progradation when accommodation decreased before the exposure of the platform (S1 surface).

Between Los Arcos and Las Canteras, coarse basement-derived alluvial-fan deposits of the Red Conglomerates covered the S1 surface (Fig. 15C). The alluvial-fan was debris-flow dominated and carried mainly pebble- to cobble-size clasts from the neighboring basin margin. The deposition of these conglomerates on the surface of subaerial exposure S1 indicates a

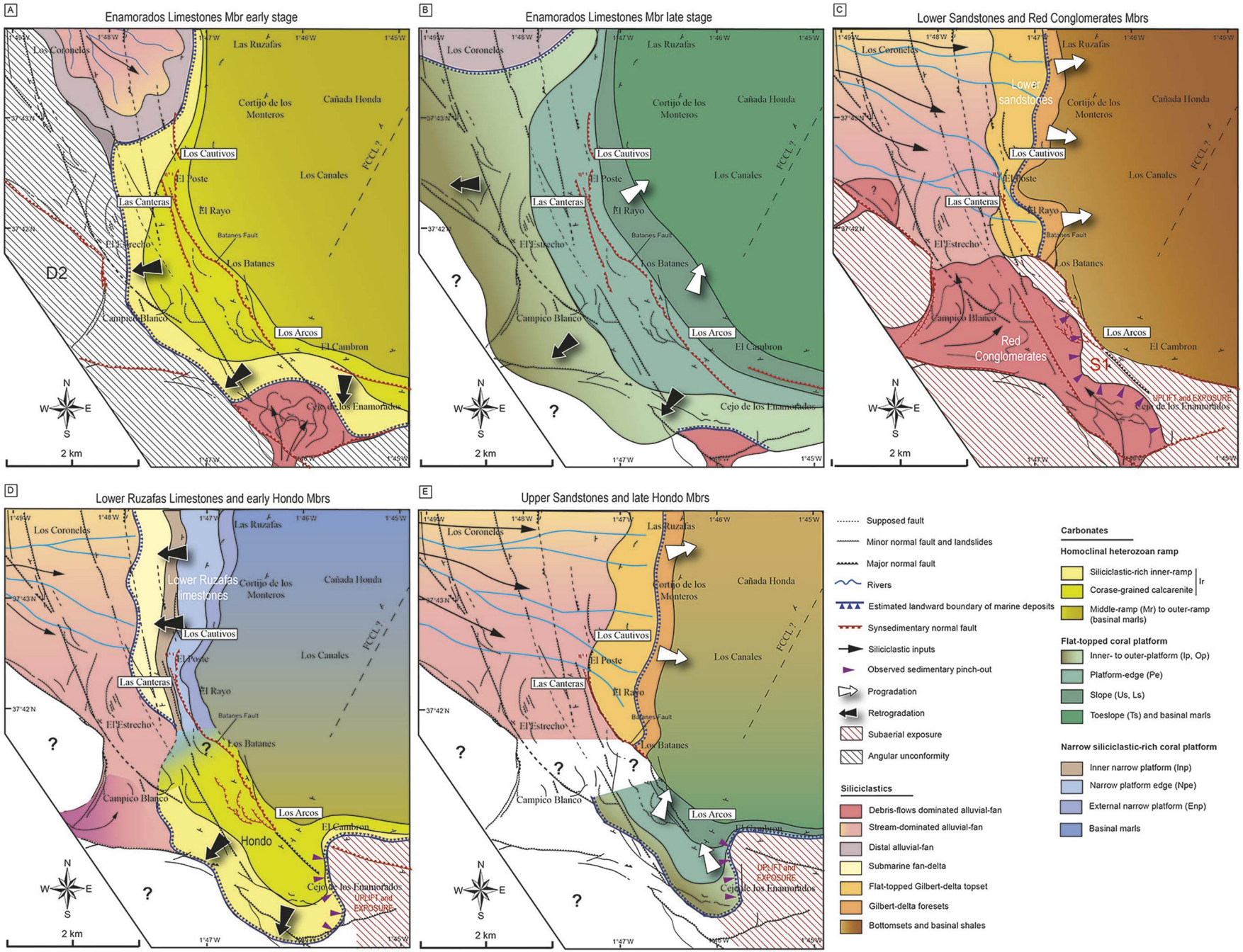


FIG. 14.—Paleogeographical maps (A to E) of the southern Lorca Basin from the deposition of the Enamorados Limestones to the Lower Ruzafas and Hondo mbrs.

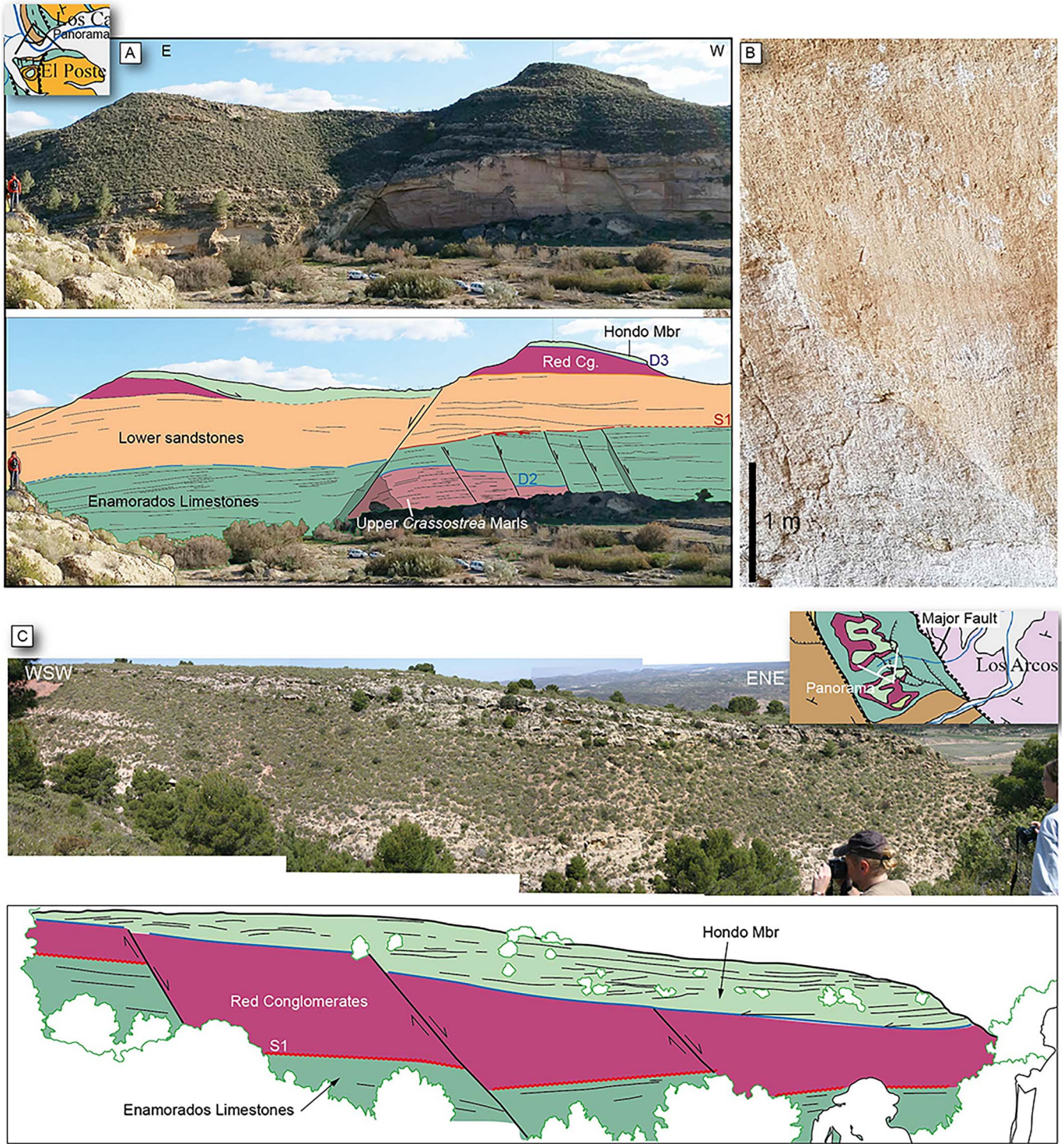


FIG. 15.—Examples of synsedimentary faults in the Lorca Basin. **A)** Synsedimentary extensional faults impacting the Enamorados Limestones Mbr in the Las Canteras area. **B)** Pure normal striae on the fault plane. **C)** Synsedimentary faults sealed by the upper part of the Hondo Mbr in the Los Arcos area.

renewal in accommodation. The conglomerates pinch out in the vicinity of the Batanes Fault (Figs. 3A, 14C) and their thickness increase southward in the direction of marginal faults. At the same time, the Red Conglomerates pinched out gradually to the southeast on the top of the Cejo de los Enamorados (Fig. 14C) as observable on the geological map in Figure 1C. As a consequence, and even if paleoflow directions cannot be measured in debris-flow deposits of the Red Conglomerates, the occurrence of highs to the NE and SE probably diverted the transport direction to the north or northwest. The volume of preserved sediments in the Red Conglomerates can be estimated to about 70 or 80 million $m^3$. In the Los Cautivos area, an extended deltaic system (Lower Sandstones) certainly fed by a large alluvial system prograded from the west (Fig. 14C). It carried local basement clasts

and exotic material from the Subbetic (Carpentier et al. 2020; Wrobel and Michalzik 1999). The grain size of the transported material ranged from shales, deposited in alluvial-plain deposits and deltaic bottomsets, to sands and pebbles accumulated in alluvial channels and deltaic foresets. The volume of siliciclastics deposited in this large alluvial and deltaic system can be estimated to more than 900 million $m^3$.

The early marine transgressive stages of the Hondo Mbr flooded the southern margin in the Los Arcos area but they pinched out to the southeast on the Cejo de los Enamorados (Fig. 14D). They are characterized by homoclinal heterozoan ramp facies covering the Red Conglomerates. In the Los Cautivos area, the Lower Ruzafas Limestones, corresponding to the lateral equivalent of the Hondo Fm, colonized the delta top and a narrow siliciclastic-rich coral platform retreated gradually landward as well as siliciclastic deposits. During the highstand, the coral platform of the upper part of the Hondo Mbr prograded northwestward in the Los Arcos area (Fig. 14E). In the Los Cautivos area, located in the axis of the deltaic system, carbonates disappeared during the highstand and were replaced by prograding deltaic siliciclastics.

### *Factors Controlling the Sequence Stratigraphic Framework of Carbonates*

A global tectonic, climatic, and eustatic control on the sequence-stratigraphic framework of carbonate production in mixed carbonate–siliciclastic systems has been proposed in several studies (e.g., Rankey et al. 1999; Bassant et al. 2005; Embry et al. 2010). Other authors favor predominantly local controls (e.g., Zecchin and Catuneanu 2017; Schwarz et al. 2018). For the Neogene basins of the Betics, the influence of climate and eustasy versus local parameters on carbonate–siliciclastic alternations and changes in benthic associations was also debated (Franseen and Mankiewicz 1991; Brachert et al. 2001, 2002; Braga et al. 2006). In the Lorca Basin, results of this study show that the sequence stratigraphic pattern of carbonate production varies between localities and with time. In addition, several carbonate depositional profiles have developed in different localities and sequence stratigraphic frameworks during the late Tortonian and the early Messinian. Therefore, several local or global factors may have controlled the initiation, persistence, or decline of carbonate production and the types of depositional profiles. They are discussed below.

**Tectonics.**—A feature common to all the studied outcrops is that the initiation of carbonate sedimentation occurred during transgressions coeval with periods of renewal in accommodation. The positive accommodation results from either local tectonics or eustasy. In other Neogene basins of the Betics, such as the Sorbas and Nijar basins, several angular unconformities between carbonate units on basin margins were recorded during the early Messinian before the onset of the evaporitic sedimentation (Martin and Braga 1994; Riding et al. 1998; Warrlich et al. 2005). Warrlich et al. (2005) interpreted these unconformities and the variations in the sequence numbers observed in these basins in comparison to the Las Negras outcrop as resulting from local tectonic control. Montgomery et al. (2001) also proposed a local tectonic control on early Messinian sedimentary cycles in the Cabo de Gata area. In addition, tectonically active zones with a stepped margin and an abrupt transition from shallow or subaerial environments to deep basin are favorable for the development of Gilbert deltas as in Los Cautivos (Postma 1990a, 1990b; Garcia-Garcia et al. 2006; Alçiçek 2007; Breda et al. 2007; Backert et al. 2010).

In the Lorca Basin, synsedimentary activity of basinal faults have been observed in several outcrops (Fig. 15). The paleogeographic maps also illuminate the possible impact of synsedimentary activities on facies distributions (Fig. 14). The D2 angular unconformity is not observed in the Los Cautivos area but is visible in the Los Arcos area near the basin margin (Fig. 16). These observations suggest that the D2 unconformity was linked to the activity of marginal faults. In the Las Canteras area, evidence of synsedimentary activity of normal faults near the Batanes Fault is apparent, as these faults cut across the Enamorados Limestones but are sealed by the Lower Sandstones (Fig. 15A, B). The Batanes Fault remained active during the highstand of the Enamorados Limestones and probably influenced the location of the platform edge during progradation (Fig. 14B).

A southward synsedimentary tilting of the substratum and the existence of a subsiding corridor between the Batanes and marginal normal faults could explain the local pinch-out of the Red Conglomerates toward the basin (Fig. 14C). Also, in the northwest of the Los Arcos valley, normal faults, corresponding to subsidiaries of the major Los Batanes Fault are sealed by deposits of the upper part of the Hondo Mbr (Fig. 15C). At the same time, the uplift of the southeastern part of the basin is attested to by the gradual disappearance and pinch-out of the Red Conglomerates on the top of the Cejo de los Enamorados. This uplift induced a decrease in accommodation that can explain the northwestward direction and reduced sigmoid progradation in the Hondo Mbr during the highstand.

However, the accommodation produced or removed by all this synsedimentary tectonics only generated local variations in thicknesses. Transgressions, highstands and lowstands are coeval in Los Arcos–Las Canteras and Los Cautivos areas (Fig. 16). It indicates that local variations in accommodation due to tectonics were not important enough to generate variations in the sequence stratigraphic evolution between different parts of the basin. This suggests, on the contrary, that a more global factor controlled transgressions and the initiation of carbonate sedimentation in the Lorca Basin.

**Eustasy.**—By comparison with the eustatic curve of Miller et al. (2011), the transgression of the Enamorados Limestones can be correlated with the eustatic rise at the Tortonian—Messinian boundary (Fig. 16). The extensive distribution of the Enamorados Limestones, their consistent sequence stratigraphy and facies evolutions in different parts of the basin on either side of the Batanes Fault, and the subaerial exposure (S1 surface) evident in all outcrops (Fig. 16) indicate that variations in accommodation in the Lorca Basin during the late Tortonian–early Messinian transition were likely controlled by eustasy.

During the early Messinian, the alternations between deltaic deposits (Lower and Upper Sandstone mbrs) and the Lower and Upper Ruzafas Limestones do not clearly match with the eustatic curve of Miller et al. (2011) (Fig. 16). As proposed by Wrobel and Michalzik (1999), this succession between siliciclastic and carbonate units could result from higher frequency (fourth-order) orbital cycles above the resolution of the eustatic curve, even if these authors noticed that "... an extrabasinal (eustatic) background control for '4th-order' cycles can only be assumed but cannot be proven by our own studies." The extensive transgression observed in the southwestern part of the Lorca Basin (Lower Ruzafas Limestones and Hondo mbrs; Fig. 16), occurring in areas with diverse tectonic evolution on either side of the Batanes Fault, and the flooding of basin margins by the Hondo Mbr (Figs. 15, 16) are rather consistent with an eustatic control on high-frequency transgressions.

**Topography *versus* Terrigenous Inputs and Carbonate Production.**—Obtained paleogeographic maps demonstrate that the tectonics of marginal faults favored the development of short, immature alluvial fans backed on the southern Lorca Basin margin or generated a steep topography marked by the D2 angular unconformity (Fig. 14). On this margin, during transgressions, the carbonate retrogradation occurred on the sloping surface formed by the unconformity (Enamorados Limestones) or by the topography formed by alluvial fans (Hondo) (Figs. 15A, 17A). Near major marginal faults, the presence of steep margins prevented the edges of the basin and sources of terrigenous material from being drowned during the initial stage of transgression (Fig. 17A). As a consequence, in such a coastal setting, siliciclastic input can remain significant during

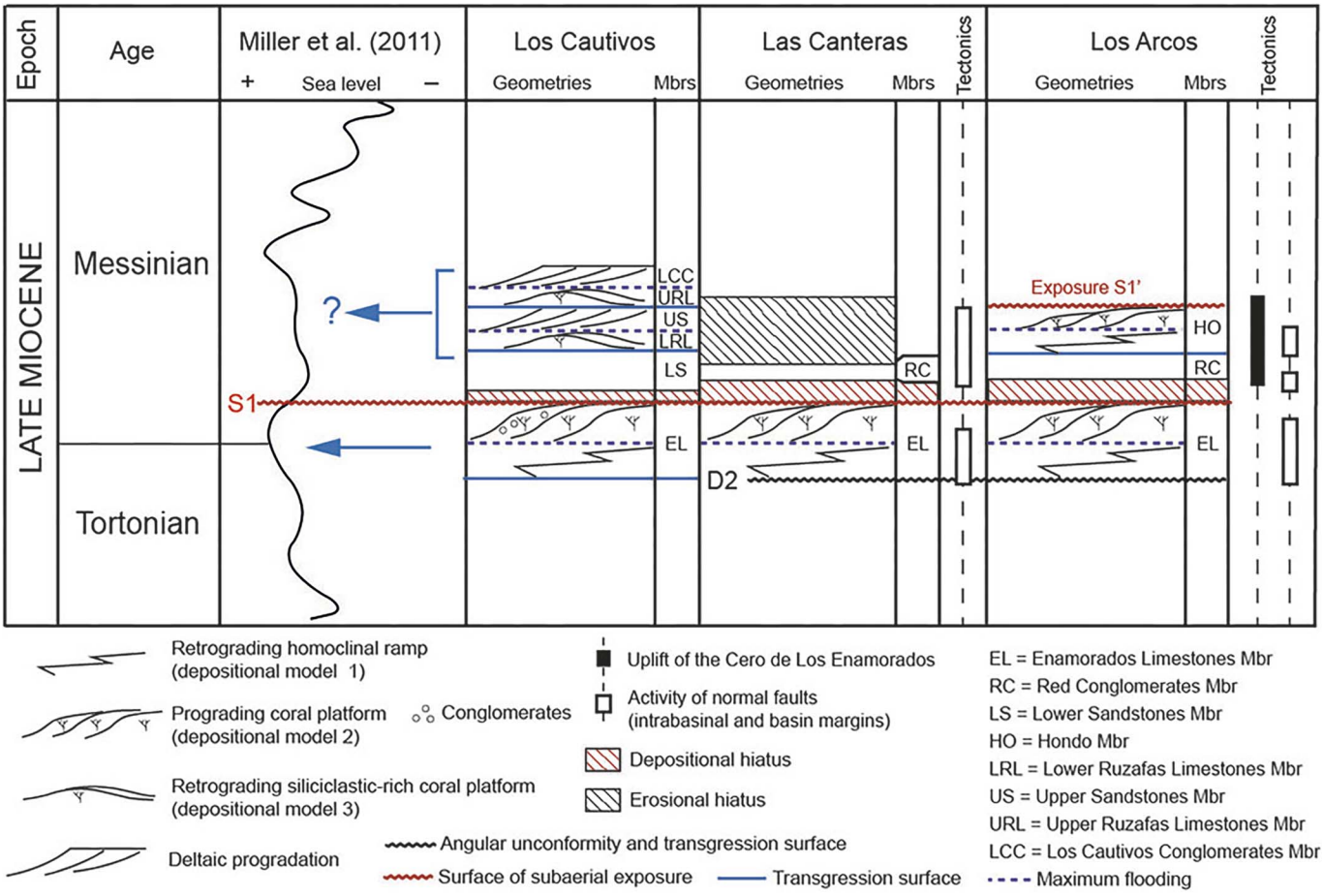


FIG. 16.—Synthesis diagram of the main surfaces, timing, and geometries of carbonate members, tectonic events, and eustatic variations in the southern Lorca Basin during the late Tortonian and early Messinian.

transgressions (Ghinassi 2007). This is supported by the significant amount of siliciclastics (about 85%) in inner-ramp facies. In addition, in the absence of benthic communities able to trap sediment at shallow depth (e.g., corals), wave action on the sea floor on the inner ramp would have remobilized the sediments, placing the fine-grained particles back in suspension and reducing depth of light penetration. Resulting deposits are thin and dominated by heterotrophic filter-feeding benthic communities composed of *Heterostegina* foraminifers, *Crassostrea gryphoides*, barnacles, and coralline algae adapted to low light levels and nutrient-rich environments (depositional model 1) (Hallock 2001; Halfar et al. 2006). The moderate rate of carbonate production generated by this kind of benthic association (Schlager 2003; Pedley and Carannante 2006; Schäfer et al. 2011; Pomar et al. 2012) was not sufficient to compensate for the eustatic increase in accommodation, and a transgression occurred. During the transgression, the progressive flooding of the small drainage basins of local immature alluvial systems led to reduction of the amount of terrigenous inputs towards the center of the basin (Fig. 17C).

At the end of the transgression, coarse siliciclastic inputs were limited, with gravel-size siliciclastic material reaching only the inner platform. In this proximal environment, the amount of siliciclastics decreased to 27%, and it diminished to less than 4% in areas ranging from the platform edge to the toe of the slope. As a consequence, at shallow depth, light conditions on the sea-floor became favorable for the installation of coral buildups.

During highstand, the trapping of carbonate sediments by constructions: 1) limited their remobilization by waves and a moderate level of turbidity certainly occurred in the platform front, and 2) favored the transition to a flat-topped geometry (Pomar et al. 2012, 2017). A classical coral zonation (depositional model 2) appeared during the basinward progradation as observed in other late Neogene settings (Perrin et al. 1995; Esteban 1996; Pomar 1996; Pomar et al. 2017). Despite a period of positive accommodation, the significant carbonate production provided by photozoan benthic associations filled the available space, as indicated by the long-term shallowing-upward trend and the sigmoid progradation in the Enamorados Limestones in the Los Arcos area (Fig. 5). In this context, a sigmoid platform progradation and coeval retrogradation on basin margin can start before the maximum accommodation rate was reached (Razin et al. 2010). The flooding of drainage basins and the resulting diminution in siliciclastic inputs continued during the highstand. Along this depositional profile type 2, light penetration at depth favored the development of coral associations, but with a limited diversity (Vennin et al. 2004). This relatively low diversity was interpreted by Sælen et al. (2016) as being the result of unstable local environmental conditions characterized by salinity and temperature fluctuations. During the late Neogene, the Betics occupied a subtropical position. This, combined with a cooling climate following the Burdigalian climax of coral development (during the late Tortonian and the Messinian in the Mediterranean area), as well as an intensification of oceanic circulation during the late Miocene, certainly impacted the diversity of coral communities (Pomar 2001; Kiessling et al. 2003; Bruch et al. 2007; Pomar and Hallock; 2008; Bosellini and Perrin 2012; Kontakiotis et al. 2019; Targhi et al. 2021).

In tectonically calm margins with large and mature drainage basins, such as in the Los Cautivos area, mature deltaic systems developed. Small

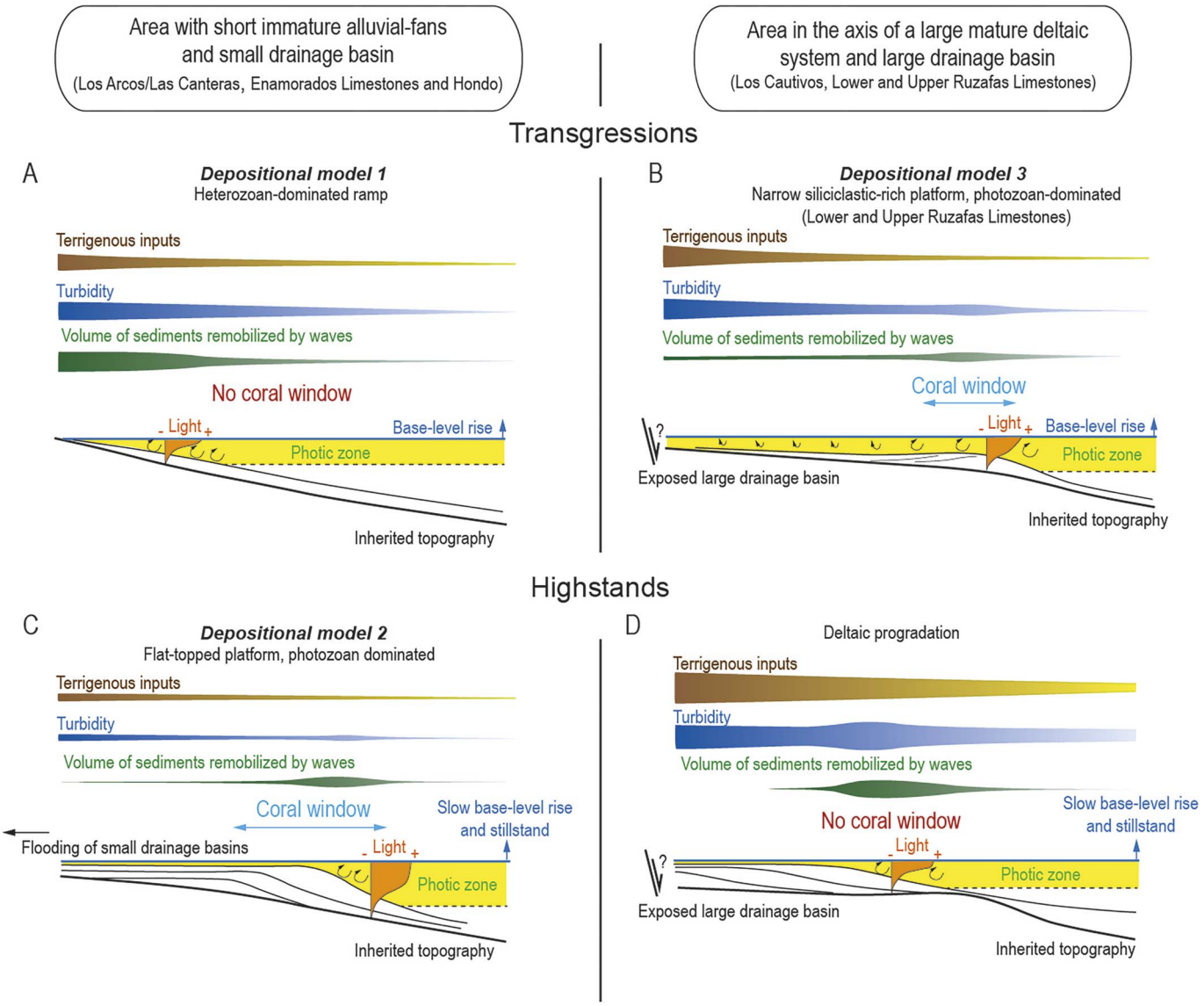


FIG. 17.—General model of the interaction between the main factors controlling the carbonate–siliciclastic alternations in the Lorca Basin.

*Porites* buildups formed on mouth bars at the top of a shoal-water delta. They constitute the first attempts of coral colonization before the deposition of the Lower and Upper Ruzafas Limestones. Despite the siliciclastic supplies, delta-front environments can favor the development of coral communities because of the renewal of marine water under high hydrodynamic conditions (Wilson and Lokier 2002; Wilson 2005). In Los Cautivos, these small coral buildups appeared during late highstands when accommodation was positive and aggradation occurred on the delta top rather than during periods of oblique progradation (Fig. 13B). The decrease in inputs of coarse siliciclastics during the initial growth of buildups suggests that part of the siliciclastic material was stored in more proximal areas of the depositional profile when accommodation increased. In addition, like in today's deltaic environments, autocyclic processes as lateral migration of distributaries probably controlled the distribution of siliciclastic sediments on the delta-front and allowed the local appearance of short-lived environmental windows for the growth of corals (Wilson and Lokier 2002; Vieira et al. 2019).

These tectonically calm margins are characterized by a relatively more important carbonate production during transgressions. Indeed, narrow siliciclastic-rich platforms (type 3) developed on the flat topography at the top of shoal-water deltas (Fig. 17B). In transgressive contexts, the retreat of terrigenous deposits is rapid on a flat topography during periods of high accommodation (Hardy 2019), and a moderate flooding can generate a significant landward shift of terrigenous sedimentation (Ghinassi 2007). The persistence of exotic coarse-grained terrigenous inputs shows that the large drainage basin was not submerged during the deposition of the Lower and Upper Ruzafas Limestones (Fig. 17F). Even if fine-grained siliciclastic inputs were still present, coarse-grained material reached the distal parts of the depositional profile only during episodic catastrophic events, as attested by the intercalation of conglomeratic debris flows within *Tarbellastraea* buildups. As a result, a shallow photic zone, affected only by fine-grained terrigenous material in suspension, can exist in the distal part of the flat inherited delta-top topography, making it suitable to the growth of specific corals (Fig. 17B). In most carbonate settings the rate of carbonate production is not uniform along the depositional

profile (Wright and Burgess 2005). For the Lower and Upper Ruzafas Limestones, the loci of the greatest carbonate production were certainly in the coral constructions of the platform edge, while production was lower in the inner-platform, which was more impacted by terrigenous inputs and probably by temperature variations induced by freshwater input (Sælen et al. 2016). The available space, which was not compensated by the low sedimentation rate in the inner-platform, was gradually filled by *Tarbellastraea* constructions during the landward migration of depositional environments.

Compared to modern tropical reefs, several features of the Upper Ruzafas Limestones suggest a low-light environment and a reduced thickness of the photic zone, as commonly observed in high-latitude settings (Halfar et al. 2005): 1) an inner platform with a significant amount of siliciclastics (78%), which diminishes to about 10% on the platform edge), 2) a dominance of encrusting forms in a siliciclastics-rich calcarenite in the internal shallow part of the depositional profile (Montaggioni and Braithwaite 2009), 3) a strong predominance of *Merulinidae* corals (Yamano et al. 2001, 2012), and 4) a rapid lateral transition from a coral-dominated environment at shallow depth to deposits dominated by heterozoan assemblages in a basinward direction (unit 2, Fig. 9A). The migration of photozoan communities towards shallow depth is an adaptation already observed in turbid and nutrient-rich environments (Wilson and Lokier 2002; Bauch et al. 2011), and is particularly true for deltaic environments (Wilson 2005). The sediments trapped by the corals were certainly not strongly remobilized by waves, and the low degree of light penetration was rather caused by the fine-grained siliciclastic sediments held in suspension supplied by the delta (Fig. 17B).

In the Lorca Basin, episodes of carbonate production alternated with significant accumulations of siliciclastic material. These two types of sedimentation also coexisted in different geographic areas, as suggested by the paleogeographic maps generated in this study. In the axis of the deltaic system high volumes of siliciclastic material entered the basin when the rate of accommodation decreased (Fig. 17D). The reduction in the surface area of carbonate production during progradation of siliciclastic deposits has been documented for numerous ancient and modern examples (Wilson and Lokier 2002; Bassant et al. 2005; Palmer et al. 2010; Bauch et al. 2011). This return of siliciclastic inputs, mostly during highstand periods, could be explained by: 1) the important size of the drainage basin of the deltaic system out of the Lorca Basin (as attested by exotic clasts in conglomerates), which was permanently exposed even after transgressions and that allowed important continuous inputs of siliciclastics, 2) an uplift of the drainage basin that generated a rejuvenation of siliciclastic sources, 3) a climatic increase in rainfall that favored erosion in the drainage basin and an efficient transport of siliciclastics to the delta front. However, the coeval persistence of carbonates during the highstand in other parts of the basin (i.e., Hondo Mbr, Los Arcos area) suggests that the return of siliciclastics in Los Cautivos area was due to a local control rather than to a global change in climate. In addition, no clear evidence of an uplift in the drainage basin of the deltaic system can be provided. As a consequence, the size of the drainage basin likely to be flooded or not during transgressions certainly constituted the main controlling parameter on the return of siliciclastics during highstands. In such a context, the sediments stored at the delta front gradually covered and buried the carbonates. While most of the siliciclastics bypassed the topsets and accumulated on the delta front, turbidity prevented the installation of autotrophic-dominated benthic communities. This is evidenced by the return of heterotrophic suspension-feeder associations such as *Ostrea edulis* and barnacles, and the absence of corals.

## CONCLUSIONS

1) Based on facies analysis and stratigraphic architecture, three different carbonate depositional models were identified in the mixed carbonate–siliciclastic sedimentary succession of the Neogene Lorca Basin (SE Spain). These models represent a heterotrophic homoclinal ramp, a flat-topped coral platform, and a narrow siliciclastics-rich coral platform.
2) Local tectonics influenced basin physiography, which controlled the entryway points, the distribution, and the volume of siliciclastic material within the basin. In addition, the preexisting local tectonic- or sedimentary-inherited topography impacted the amount of siliciclastics in the photic zone at the onset of transgressions.
3) Each depositional model preferentially developed during either transgressions or highstands, making a basic application of Walther's Law difficult in this mixed carbonate–siliciclastic system. The carbonate production systematically started during transgressions. The global distribution of the transgressive carbonates at the basin scale shows that eustatic control governed variations in accommodation.
4) Carbonate production was modulated according to specific phases of the relative sea-level cycle and inherited topography. During the transgression, maximum carbonate production occurred through either: a) a heterotrophic community developing on a ramp over a steep substratum with overall moderate terrigenous input, or b) low-diversity coral buildups in siliciclastics-rich environments on a flat deltaic topography. During highstands, steep margins were subject to low terrigenous flow because of the submersion of local siliciclastic sources during previous transgressions. Flat-topped carbonate coral platforms were able to prograde basinward and to retrograde on basin margins simultaneously. In contrast, if the drainage area of siliciclastic systems was large and permanently exposed even after transgressions, a large volume of siliciclastic material entered the basin during the highstand period. In this scenario, carbonates developed only during transgressions before being buried by siliciclastics during highstands.

## ACKNOWLEDGMENTS

This study was supported by the CNRS–INSU (Centre National de la Recherche Scientifique–Institut National des Sciences de l'Univers) as part of the SYSTER (Système Terre: processus et couplages) action. We are grateful to G. Warrlich and an anonymous reviewer for their remarks and comments. We would also like to thank Editor S. Kaczmarek. We thank Bernard Lathuilière for his advice and corrections of the manuscript. We are grateful to Gregorio Francisco Martinez Rodriguez for his material and logistical help during field missions and Aurélien Eglinger for his company in the field and his role as scale on some images.

## DATA AVAILABILITY

The data that support the findings of this study are available from the corresponding author upon reasonable request.

## SUPPLEMENTAL MATERIALS

Supplemental materials are available from the SEPM Data Archive: https://www.sepm.org/supplemental-materials.

## REFERENCES

Alçiçek, M.C., 2007, Tectonic development of an orogen-top rift recorded by its terrestrial sedimentation pattern: the Neogene Eşen Basin of southwestern Anatolia, Turkey: Sedimentary Geology, v. 200, p. 117–140.

Augier, R., Jolivet, L., and Robin, C., 2005, Late orogenic doming in the eastern Betic Cordilleras: final exhumation of the Nevado–Filabride complex and its relation to basin genesis: Tectonics, v. 24, TC4003, doi:10.1029/2004TC001687.

Augier, R., Jolivet, L., Do Couto, D., and Negro, F., 2013, From ductile to brittle, late- to post-orogenic evolution of the Betic Cordillera: structural insights from the northeastern Internal zones: Société Géologique de France, Bulletin, v. 184, p. 405–425.

Backert, N., Ford, M., and Malartre, F., 2010, Architecture and sedimentology of the Kerinitis Gilbert-type fan delta, Corinth Rift, Greece: Sedimentology, v. 57, p. 543–586.

Bassant, P., van Buchem, F.S.P., Strasser, A., and Görür, N., 2005, The stratigraphic architecture and evolution of the Burdigalian carbonate–siliciclastic sedimentary systems of the Mut Basin, Turkey: Sedimentary Geology, v. 173, p. 187–232.

Bauch, T., Reijmer, J., McNeill, D., and Schäfer, P., 2011, Development of a Pliocene mixed carbonate–siliciclastic reef (Limon, Costa Rica): Sedimentary Geology, v. 239, p. 37–47.

Betzler, C., Brachert, T.C., Braga, J., and Martin, J.M., 1997, Nearshore, temperate, carbonate depositional systems (lower Tortonian, Agua Amarga Basin, southern Spain): implications for carbonate sequence stratigraphy: Sedimentary Geology, v. 113, p. 27–53.

Betzler, C., Fürstenau, J., Lüdmann, T., Hübscher, C., Lindhorst, S., Paul, A., Reijmer, J., and Droxler, A., 2012, Sea-level and ocean-current control on carbonate-platform growth, Maldives, Indian Ocean: Basin Research, v. 24, p. 1–25.

Booth-Rea, G., Garcia-Duenas, V., and Azanon, J.M., 2002, Extensional attenuation of the malaguide and Alpujarride thrust sheets in a segment of the Alboran basin folded during the Tortonian (Lorca area, Eastern Betics): Comptes Rendus Geosciences, v. 334, p. 557–563.

Booth-Rea, G., Azanon, J.M., Garcia-Duenas, V., and Augier, R., 2003, Uppermost Tortonian to Quaternary depocentre migration related with segmentation of the strike-slip Palomares Fault Zone, Vera Basin (SE Spain): Comptes Rendus Geosciences, v. 335, p. 751–761.

Booth-Rea, G., Azanon, J.M., and Garcia-Duenas, V., 2004, Extensional tectonics in the northeastern Betics (SE Spain): case study of extension in a multilayered upper crust with contrasting rheologies: Journal of Structural Geology, v. 26, p. 2039–2058.

Bosence, D., 1983, The occurrence and ecology of recent rhodoliths: a review, *in* Peryt, T., ed., Coated Grains: Springer-Verlag, p. 225–242.

Bosence, D., 2005, A genetic classification of carbonate platforms based on their basinal and tectonic settings in the Cenozoic: Sedimentary Geology, v. 175, p. 49–72.

Bosellini, F.R., and Perrin, C., 2012, Coral diversity and temperature: a palaeoclimatic perspective for the Oligo-Miocene of the Mediterranean region, *in* Mutti, M., Piller, W., and Betzler, C., eds., Carbonate Systems during the Oligocene–Miocene Climatic Transition: International Association of Sedimentologists, Special Publication 42, p. 229–244.

Bourillot, R., Vennin, E., Rouchy, J.M., Durlet, C., Rommevaux, V., Kolodka, C., and Knap, F., 2009, Structure and evolution of a Messinian mixed carbonate–siliciclastic platform: the role of evaporites (Sorbas Basin, South-east Spain): Sedimentology, v. 57, p. 477–512.

Bourillot, R., Vennin, E., Rouchy, J.M., Blanc-Valleron, M.M., Caruso, A., and Durlet, C., 2010, The end of the Messinian Salinity Crisis in the western Mediterranean: insights from the carbonate platforms of south-eastern Spain: Sedimentary Geology, v. 229, p. 224–253.

Brachert, T., Hultzsch, N., Knoerich, A., Krautworst, U., and Stückrad, O., 2001, Climatic signatures in shallow-water carbonates: high-resolution stratigraphic markers in structurally controlled carbonate buildups (Late Miocene, southern Spain): Palaeogeography, Palaeoclimatology, Palaeoecology, v. 175, p. 211–237.

Brachert, T., Krautworst, U., and Stueckrad, O., 2002, Tectono-climatic evolution of a Neogene intramontane basin (Late Miocene Carboneras subbasin, southeast Spain): revelations from basin mapping and biofacies analysis: Basin Research, v. 14, p. 503–521.

Braga, J., and Aguirre, J., 2001, Coralline algal assemblages in upper Neogene reef and temperate carbonates in Southern Spain: Palaeogeography, Palaeoclimatology, Palaeoecology, v. 175, p. 27–41.

Braga, J., and Martin, J., 1988, Neogene coralline-algal growth-forms and their palaeoenvironments in the Almanzora river valley (Almeria, S.E. Spain): Palaeogeography, Palaeoclimatology, Palaeoecology, v. 67, p. 285–303.

Braga, J., and Martin, J., 1996, Geometries of reef advance in response to relative sea-level changes in a Messinian (uppermost Miocene) fringing reef (Cariatiz reef, Sorbas Basin, SE Spain): Sedimentary Geology, v. 107, p. 61–81.

Braga, J., Martin, J., and Wood, J., 2001, Submarine lobes and feeder channels of redeposited, temperate carbonate and mixed siliciclastic–carbonate platform deposits (Vera Basin, Almeria, southern Spain): Sedimentology, v. 48, p. 99–116.

Braga, J., Martin, J., Betzler, C., and Aguirre, J., 2006, Models of temperate carbonate deposition in Neogene basins in SE Spain: a synthesis, *in* Pedley, H.M., and Carannante, G., eds., Cool-Water Carbonates: Depositional Systems and Palaeoenvironmental Controls: Geological Society of London, Special Publication 255, p. 121–135.

Brandano, M., Bosselini, F., Mazzucchi, A., and Tomassetti, L., 2016, Coral assemblages and bioconstructions adapted to the depositional dynamics of a mixed carbonate–siliciclastic setting: the case study of the Burdigalian Bonifacio Basin (south Corsica): Rivista Italiana di Paleontologia e Stratigrafia, v. 122, p. 37–52.

Breda, A., Mellere, D., and Massari, F., 2007, Facies and processes in a Gilbert-delta-filled incised valley (Pliocene of Ventimiglia, NW Italy): Sedimentary Geology, v. 200, p. 31–55.

Bruch, A.A., Uhl, D., and Mosbrugger, V., 2007, Miocene climate in Europe–patterns and evolution: a first synthesis of NECLIME: Palaeogeography, Palaeoclimatology, Palaeoecology, v. 253, p. 1–7.

Burchette, T.P., and Wright, V.P., 1992, Carbonate ramp depositional systems: Sedimentary Geology, v. 79, p. 3–57.

Carpentier, C., Lathuilière, B., and Ferry, S., 2010, Sequential and climatic framework of the growth and demise of a carbonate platform: implications for the peritidal cycles (Late Jurassic, north-eastern France): Sedimentology, v. 57, p. 985–1020.

Carpentier, C., Vennin, E., Rouchy, J.M., Cornee, J.J., Melinte-Dobrinescu, M., Hibsch, C., Olivier, N., Caruso, A., and Bartier, D., 2020, Ages and stratigraphical architecture of late Miocene deposits in the Lorca Basin (Betics, SE Spain): new insights for the salinity crisis in marginal basins: Sedimentary Geology, v. 405, doi:10.1016/j.sedgeo.2020.105700.

Catuneanu, O., Abreu, V., Bhattacharya, J.P., Blum, M.D., Dalrymple, R.W., Eriksson, P.G., Fielding, C.R., Fisher, W.L., Galloway, W.E., Gibling, M.R., Giles, K.A., Holbrook, J.M., Jordan, R., Kendall, C.G.St.C., Macurda, B., Martinsen, O.J., Miall, A.D., Neal, J.E., Nummedal, D., Pomar, L., Posamentier, H.W., Pratt, B.R., Sarg, J.F., Shanley, K.W., Steel, R.J., Strasser, A., Tucker, M.E., and Winker, C., 2009, Towards the standardization of sequence stratigraphy: Earth-Science Reviews, v. 92, p. 1–33.

Chalouan, A., Saji, R., Michard, A., and Bally, A., 1997, Neogene tectonic evolution of the southern Alboran basin as inferred from seismic data of Morocco: American Association of Petroleum Geologists, Bulletin, v. 81, p. 1161–1184.

Chazottes, V., Reijmer, J., and Cordier, E., 2008, Sediment characteristics in reef areas influenced by eutrophication-related alterations of benthic communities and bioerosion processes: Marine Geology, v. 250, p. 114–127.

Cloetingh, S., van der Beek, P.A., van Rees, D., Roep, T.B., Biermann, C., and Stephenson, R.A., 1992, Flexural interaction and the dynamics of Neogene extensional basin formation in the Alboran–Betic region: Geo-Marine Letters, v. 12, p. 66–75.

Coffey, B.P., and Read, J.F., 2004, Mixed carbonate–siliciclastic sequence stratigraphy of a Paleogene transition zone continental shelf, southeastern USA: Sedimentary Geology, v. 166, p. 21–57.

Comas, M., Garcia-Duenas, V., and Jurado, M., 1992, Neogene tectonic evolution of the Alboran Sea from MCS data: Geo-Marine Letters, v. 12, p. 157–164.

Corrochano, D., Barba, P., and Colmenero, J.R., 2012, Glacioeustatic cyclicity of a Pennsylvanian carbonate platform in a foreland basin setting: an example from the Bachende Formation of the Cantabrian Zone (NW Spain): Sedimentary Geology, v. 245, p. 76–93.

D'Agostini, D.P., Bastos, A.C., and Dos Reis, A.T., 2015, The modern mixed carbonate–siliciclastic Abrolhos Shelf: implications for a mixed depositional model: Journal of Sedimentary Research, v. 85, p. 124–139.

Daniell, J., Manoy, T., Beaman, R.J., Webster, J.M., and Puga-Bernabéu, A., 2020, Shelf-edge delta and reef development on a mixed siliciclastic–carbonate margin, central Great Barrier reef: Journal of Sedimentary Research, v. 90, p. 1286–1304.

Dercourt, J., Zonenshain, L.P., Ricou, L.E., Kazmin, V.G., Le Pichon, X., Knipper, A.L., Grandjacquet, C., Shotshikov, I.M., Geyssant, J., Lepvrier, C., Perchersky, D.H., Boulin, J., Sibuet, J.C., Savostin, L.A., Sorokhtin, O., Westphal, M., Bazhenov, M.L., Lauer, J.P., and Bijou-Duval, B., 1986, Geological evolution of the Tethys belt from the Atlantic to the Pamirs since the Lias: Tectonophysics, v. 123, p. 241–315.

Do Couto, D., Gumiaux, C., Augier, R., Lebret, N., Folcher, N., Jouannic, G., Jolivet, L., Suc, J.P., and Gorini, C., 2014, Tectonic inversion of an asymmetric graben: insights from a combined field and gravity survey in the Sorbas basin: Tectonics, v. 33, p. 1360–1385.

Do Couto, D., Gorini, C., Jolivet, L., Lebret, N., Augier, R., Gumiaux, C., d'Acremont, E., Ammar, A., Jabour, H., and Auxietre, J.L., 2016, Tectonic and stratigraphic evolution of the Western Alboran Sea Basin in the last 25 Myrs: Tectonophysics, v. 677–678, p. 280–311.

Embry, J.C., Vennin, E., Van Buchem, F.S.P., Schroeder, R., Pierre, C., and Aurell, M., 2010, Sequence stratigraphy and carbon isotope stratigraphy of an Aptian mixed carbonate–siliciclastic platform to basin transition (Galve sub-basin, NE Spain), *in* van Buchem, F.S.P., Gerdes, K.D., and Esteban, M., eds., Mesozoic and Cenozoic Carbonate Systems of the Mediterranean and the Middle East: Stratigraphic and Diagenetic Reference Models: Geological Society of London, Special Publication 329, p. 113–143.

Emery, D., and Myers, K.J., 1996, Sequence Stratigraphy: Blackwell Science, Oxford, 297 p.

Esteban, M., 1996, An overview of Miocene reefs from Mediterranean areas: general trends and facies models, *in* Franseen, E., Esteban, M., Ward, W., and Rouchy, J.M., eds., Models for Carbonate Stratigraphy from Miocene Reef Complexes of Mediterranean Regions: SEPM, Concepts in Sedimentology and Paleontology 5, p. 3–53.

Franseen, E., and Mankiewicz, C., 1991, Depositional sequences and correlation of middle(?) to late Miocene carbonate complexes, Las Negras and Nijar areas, southeastern Spain: Sedimentology, v. 38, p. 871–898.

Franseen, E.K., Goldstein, R.H. and Farr, M.R., 1997, Substrate-slope and temperature controls on carbonate ramps: revelations from Upper Miocene Outcrops, SE Spain, *in* James, N.P., and Clarke, J.A.D., eds., Cool-Water Carbonates: SEPM, Special Publication 56, p. 271–292.

Frizon de Lamotte, D., Guézou, J.C., and Albertini, M.A., 1989, Deformation related to Miocene westward translation in the core of the Betic zone: implications on the tectonic interpretation of the Betic orogen (Spain): Geodinamica Acta, v. 3, p. 267–281.

Galindo-Zaldivar, J., Gonzalez-Lodeiro, F., and Jabaloy, A., 1993, Stress and paleaostress in the Betic-rif cordilleras (Miocene to the present): Tectonophysics, v. 227, p. 105–126.

Garcia-Garcia, F., Fernandez, J., Viseras, C., and Soria, J.M., 2006, High frequency cyclicity in a vertical alternation of Gilbert-type deltas and carbonate bioconstructions in the late Tortonian, Tabernas Basin, Southern Spain: Sedimentary Geology, v. 192, p. 123–139.

Ghinassi, M., 2007, The effects of differential subsidence and coastal topography on high-order transgressive–regressive cycles: Pliocene nearshore deposits of the Val d'Orcia Basin, Northern Apennines, Italy: Sedimentary Geology, v. 202, p. 677–701.

Giaconia, F., Booth-Rea, G., Martínez-Martínez, J.M., Azañón, J.M., and Pérez-Peña, J.V., 2012, Geomorphic analysis of the Sierra Cabrera, an active pop-up in the constrictional domain of conjugate strike-slip faults: the Palomares and Polopos fault zones (eastern Betics, SE Spain): Tectonophysics, v. 580, p. 27–42.

Giaconia, F., Booth-Rea, G., Martinez-Martinez, J.M., Azanon, J.M., Storti, F., and Artoni, A., 2014, Heterogeneous extension and the role of transfer faults in the development of the southeastern Betic basins (SE Spain): Tectonics, v. 33, p. 2467–2489.

Guillen Mondejar, F., Rodriguez Estrella, T., Arana, R., and Lopez Aguayo, F., 1995, Historia geologica de la cuenca de Lorca (Murcia): influencia de la tectonica en la sedimentation: Geogaceta, v. 18, p. 30–33.

Halfar, J., Godinez-Orta, L., Riegl, B., Valdez-Holguin, J.E., and Borges, J.M., 2005, Living on the edge: high-latitude *Porites* carbonate production under temperate eutrophic conditions: Coral Reefs, v. 24, p. 582–592.

Halfar, J., Godinez-Orta, L., Mutti, M., Valdez-Holguins, J.E., and Borges, J.M., 2006, Carbonates calibrated against oceanographic parameters along a latitudinal transect in the Gulf of California, Mexico: Sedimentology, v. 53, p. 297–320.

Hallock, P., 2001, Coral reefs, carbonate sediments, nutrients, and global change, *in* Stanley G., Jr., ed., The History and Sedimentology of Ancient Reef Systems: Kluwer Academic/Plenum Publishers, p. 387–427.

Hallock, P., and Schlager, W., 1986, Nutrient excess and the demise of coral reefs and carbonate platforms: Palaios, v. 1, p. 389–398.

Hardy, S., 2019, Novel discrete element modelling of Gilbert-type delta formation in an active tectonic setting: first results: Basin Research, v. 31, p. 77–91.

Heap, A.D., Dickens, G.R., Stewart, L.K., and Woolfe, K.J., 2002, Holocene storage of siliciclastic sediment around islands on the middle shelf of the Great Barrier Reef Platform, north-east Australia: Sedimentology, v. 49, p. 603–621.

Homewood, P.W., 1996, The carbonate feedback system: interaction between stratigraphic accommodation, ecological succession and the carbonate factory: Société Géologique de France, Bulletin, v. 167, p. 701–715.

Hunt, D., and Tucker, M.E., 1992, Stranded parasequences and the forced regressive wedge systems tract: deposition during base-level fall: Sedimentary Geology, v. 81, p. 1–9.

Iribarren, L., Verges, J., Camurri, F., Fullea, J., and Fernandez, M., 2007, The structure of the Atlantic–Mediterranean transition zone from the Alboran Sea to the Horseshoe abyssal Plain (Iberia–Africa plate boundary): Marine Geology, v. 243, p. 97–119.

Isern, A.R., McKenzie, J.A., and Feary, D.A., 1996, The role of sea-surface temperature as a control on carbonate platform development in the western Coral Sea: Palaeogeography, Palaeoclimatology, Palaeoecology, v. 124, p. 247–272.

Jimenez, A., Braga, J., and Martin, J., 1991, Oyster distribution in the Upper Tortonian of the Almanzora corridor (Almeria, S.E. Spain): Geobios, v. 24, p. 725–734.

Johnson, C., Franseen, E., and Goldstein, R., 2005, The effects of sea level and palaeotopography on lithofacies distribution and geometries in heterozoan carbonates, south-eastern Spain: Sedimentology, v. 52, p. 513–536.

Kiessling, W., Flügel, E., and Golonka, J., 2003, Patterns of Phanerozoic carbonate platform sedimentation: Lethaia, v. 36, p. 195–226.

Kontakiotis, G., Besiou, E., Antonarakou, A., Zarkogiannis, S.D., Kostis, A., Mortyn, P.G., Cornée, J.J., Schulbert, C., Drinia, H., Anastasakis, G., and Karakitsios, V., 2019, Decoding sea surface and paleoclimate conditions in the eastern Mediterranean over the Tortonian–Messinian transition: Palaeogeography, Palaeoclimatology, Palaeoecology, v. 534, doi:10.1016/j.palaeo.2019.109312.

Lukasik, J., and James, N., 2006, Carbonate sedimentation, climate change and stratigraphic completeness on a Miocene cool-water epeiric ramp, Murray Basin, South Australia, *in* Pedley, H.M., and Carannante, G., eds., Cool-Water Carbonates: Depositional Systems and Palaeoenvironmental Controls: Geological Society of London, Special Publication 255, p. 217–244.

Martin, J., and Braga, J.C., 1994, Messinian events in the Sorbas Basin in southeastern Spain and their implications in the recent history of the Mediterranean: Sedimentary Geology, v. 90, p. 257–268.

Martin, J., Braga, J., Betzler, C., and Brachert, T., 1996, Sedimentary model and high-frequency cyclicity in a Mediterranean, shallow-shelf, temperate-carbonate environment (uppermost Miocene, Agua Amarga Basin, Southern Spain): Sedimentology, v. 43, p. 263–277.

Martin-Chivelet, J., 1995, Sequence stratigraphy of mixed carbonate–siliciclastic platforms developed in a tectonically active setting, Upper Cretaceous, Betic continental margin (Spain): Journal of Sedimentary Research, v. 65, p. 235–254.

Martin-Garin, B., and Montaggioni, L.F., 2023, Corals and Reefs: From the Beginning to an Uncertain Future: Springer, 174 p.

Martin-Garin, B., Lathuilière, B., and Geister, J., 2012, The shifting biogeography of reef corals during the Oxfordian (Late Jurassic). A climatic control?: Palaeogeography, Palaeoclimatology, Palaeoecology, v. 365–366, p. 136–153.

Martinez-Diaz, J., 2002, Stress-field variation related to fault interaction in a reverse oblique-slip fault: the Alhama de Murcia fault, Betic Cordillera, Spain: Tectonophysics, v. 356, p. 291–305.

Martinez-Martinez, J., Booth-Rea, G., Azanon, J.M., and Torcal, F., 2006, Active transfer fault zone linking a segmented extensional system (Betics, southern Spain): insight into heterogeneous extension driven by edge delamination: Tectonophysics, v. 422, p. 159–173.

Massari, F., and Parea, G., 1990, Wave-dominated Gilbert-type gravel delta in the hinterland of the Gulf of Taranto (Pleistocene, southern Italy), *in* Colella, A., and Prior, D., eds., Coarse Grained Deltas: International Association of Sedimentologists, Special Publication 10, p. 311–331.

Masse, J.P., and Fenerci-Masse, M., 2013, Drowning events, development and demise of carbonate platforms and controlling factors: the Late Barremian–Early Aptian record of Southeast France: Sedimentary Geology, v. 298, p. 28–52.

McConnico, T.S., and Bassett, K.N., 2007, Gravelly Gilbert-type fan delta on the Conway Coast, New Zealand: foreset depositional processes and clast imbrications: Sedimentary Geology, v. 198, p. 147–166.

Meijninger, B.M.L., and Vissers, R.L.M., 2006, Miocene extensional basin development in the Betic Cordillera, SE Spain revealed through analysis of the Alhama de Murcia and Crevillente Faults: Basin Research, v. 18, p. 547–571.

Miall, A., 2006, The Geology of Fluvial Deposits: Sedimentary Facies, Basin Analysis, and Petroleum Geology: Springer-Verlag, 582 p.

Michel, J., Borgomano, J., and Reijmer, J.J., 2018, Heterozoan carbonates: When, where and why? A synthesis on parameters controlling carbonate production and occurrences: Earth-Science Reviews, v. 182, p. 50–67.

Miller, K., Mountain, G., Wright, J., and Browning, J., 2011, A 180-million-year record of sea-level and ice volume variations from continental margin and deep-sea isotopic records: Oceanography, v. 24, p. 40–53.

Montaggioni, L.F., and Braithwaite, C.J., 2009, Quaternary Coral Reef Systems: History, Development Processes and Controlling Factors: Elsevier, Developments in Marine Geology 5, 550 p.

Montenat, C., 1996, The Betic Neogene basins: introduction, *in* Friend, P.F., and Dabrio, C., eds., Tertiary Basins of Spain: The Stratigraphic Record of Crustal Kinematics: Cambridge University Press, p. 321–322.

Montenat, C., and Ott d'Estevou, P., 1996, Late Neogene basins evolving in the Eastern Betic transcurrent fault zone: an illustrated review, *in* Friend, P.F., and Dabrio, C., eds., Tertiary Basins of Spain: The Stratigraphic Record of Crustal Kinematics: Cambridge University Press, p. 372–386.

Montenat, C., and Ott d'Estevou, P., 1999, The diversity of Late Neogene sedimentary basins generated by wrench faulting in the eastern Betic cordillera, SE Spain: Journal of Petroleum Geology, v. 22, p. 61–80.

Montenat, C., Ott d'Estevou, P., and Pierson D'Autrey, L., 1996, Miocene basins of the eastern Prebetic Zone: some tectono-sedimentary aspects, *in* Friend, P.F., and Dabrio, C., eds., Tertiary Basins of Spain: the Stratigraphic Record of Crustal Kinematics: Cambridge University Press, p. 346–352.

Montgomery, P., Farr, M.R., Franseen, E.K., and Goldstein, R.H., 2001, Constraining controls on carbonate sequences with high-resolution chronostratigraphy: Upper Miocene, Cabo de Gata region, SE Spain: Palaeogeography, Palaeoclimatology, Palaeoecology, v. 176, p. 11–45.

Mutti, E., Tinterri, R., Di Biase, D., Fava, L., Mavilla, N., Angella, S., and Calabrese, L., 2000, Delta-front facies associations of ancient flood-dominated fluvio-deltaic systems: Revista de la Sociedad Geológica de España, v. 13, p. 165–190.

Mutti, E., Tinterri, R., Benevelli, G., di Biase, D., and Cavanna, G., 2003, Deltaic, mixed and turbidite sedimentation of ancient foreland basins: Marine and Petroleum Geology, v. 20, 733–755.

Mutti, M., and Hallock, P., 2003, Carbonate systems along nutrient and temperature gradients: some sedimentological and geochemical constraints: International Journal of Earth Sciences, v. 92, p. 465–475.

Navarrete, R., Rodríguez-López, J.P., Liesa, C.L., Soria, A.R., and Fernanda de Mesquita, L.V., 2013, Changing physiography of rift basins as a control on the evolution of mixed siliciclastic–carbonate back-barrier systems (Barremian Iberian Basin, Spain): Sedimentary Geology, v. 289, p. 40–61.

Nemec, W., 1990, Aspects of sediment movements on steep delta slopes, *in* Colella, A., and Prior, D., eds., Coarse Grained Deltas: International Association of Sedimentologists, Special Publication 10, p. 29–73.

Olivier, N., Carpentier, C., Martin-Garin, B., Lathuilière, B., Gaillard, C., Ferry, S., Hantzpergue, P., and Geister, J., 2004, Coral–microbialite reefs in pure carbonate versus mixed carbonate–siliciclastic depositional environments: the example of the Pagny-sur-Meuse section (Upper Jurassic, Northeastern France): Facies, v. 50, p. 229–255.

Olivier, N., Cariou, E., and Hantzpergue, P., 2015, Evolution of a Late Oxfordian: early Kimmeridgian carbonate platform, French Jura Mountains: Swiss Journal of Geosciences, v. 108, p. 273–288.

Orton, G., and Reading, H., 1993, Variability of deltaic processes in terms of sediment supply, with particular emphasis on grain size: Sedimentology, v. 40, p. 475–512.

Palmer, S.E., Perry, C., Smithers, S., and Gulliver, P., 2010, Internal structure and accretionary history of a nearshore, turbid-zone coral reef: Paluma Shoals, central Great Barrier Reef, Australia: Marine Geology, v. 276, p. 14–29.

Paul, A., Reijmer, J., Fürstenau, J., Kinkel, H., and Betzler, C., 2012, Relationship between Late Pleistocene sea-level variations, carbonate platform morphology and aragonite production (Maldives, Indian Ocean): Sedimentology, v. 59, p. 1640–1658.

Pedley, M., and Carannante, G., 2006, Cool-water carbonate ramps: a review, *in* Pedley, M., and Carannante, G., eds., Cool Water Carbonates: Depositional Systems and Palaeoenvironmental Controls: Geological Society of London, Special Publication 255, p. 1–9.

Perrin, C., Bosence, D., and Rosen, B., 1995, Quantitative approaches to palaeozonation and palaeobathymetry of corals and coralline algae in Cenozoic reefs, *in* Bosence, D., and Allison, P., eds., Marine Palaeoenvironmental Analysis from Fossils: Geological Society of London, Special Publication 83, p. 181–229.

Philip, J.M., and Airaud-Crumiere, C., 1991, The demise of the rudist-bearing carbonate platforms at the Cenomanian–Turonian boundary: a global control: Coral Reefs, v. 10, p. 115–125.

Platt, J.P., 2007, From orogenic hinterlands to Mediterranean-style back-arc basins: a comparative analysis: Geological Society of London, Journal, v. 164, p. 297–311.

Plint, A.G., and Nummedal, D., 2000, The falling stage systems tract: recognition and importance in sequence stratigraphic analysis, *in* Hunt, D., and Gawthorpe, R.L., eds., Sedimentary Responses to Forced Regressions: Geological Society of London, Special Publication 172, p. 1–17.

Pomar, L., 1996, Upper Miocene reef complex of the Llucmajor area, Mallorca, Spain, *in* Franseen, E., Esteban, M., Ward, W., and Rouchy, J.M., eds., Models for Carbonate Stratigraphy from Miocene Reef Complexes of Mediterranean Regions: SEPM, Concepts in Sedimentology and Paleontology 5, p. 191–225.

Pomar, L., 2001, Types of carbonate platforms: a genetic approach: Basin Research, v. 13, p. 313–334.

Pomar, L., and Hallock, P., 2008, Carbonate factories: a conundrum in sedimentary geology: Earth-Science Reviews, v. 87, p. 134–169.

Pomar, L., and Ward, W.C., 1999, Reservoir-scale heterogeneity in depositional packages and diagenetic patterns on a reef-rimmed platform, upper Miocene, Mallorca, Spain: American Association of Petroleum Geologists, Bulletin, v. 83, p. 1759–1773.

Pomar, L., Brandano, M., and Westphal, H., 2004, Environmental factors influencing skeletal grain sediment associations: a critical review of Miocene examples from the western Mediterranean: Sedimentology, v. 51, p. 627–651.

Pomar, L., Bassant, P., Brandano, M., Ruchonnet, C., and Janson, X., 2012, Impact of carbonate-producing biota on platform architecture: insight from Miocene examples of the Mediterranean region: Earth-Science Reviews, v. 113, p. 186–211.

Pomar, L., Baceta, J., Hallock, P., and Mateu-Vicens, G., 2017, Reef building and carbonate production modes in the west-central Tethys during the Cenozoic: Marine and Petroleum Geology, v. 83, p. 261–304.

Posamentier, H.W., and Allen, G.P., 1999, Siliciclastic Sequence Stratigraphy: Concepts and Applications: SEPM, Concepts in Sedimentology and Paleontology 7, 216 p.

Postma, G., 1990a, An analysis of the variation in delta architecture: Terra Nova, v. 2, p. 124–130.

Postma, G., 1990b, Depositional architecture and facies of river and fan deltas: a synthesis, *in* Colella, A., and Prior, D., eds., Coarse Grained Deltas: International Association of Sedimentologists, Special Publication 10, p. 13–27.

Postma, G., Nemec, W., and Kleinspehn, K.L., 1988, Large floating clasts in turbidites: a mechanism for their emplacement: Sedimentary Geology, v. 58, p. 47–61.

Pratt, B.R., and James, N.P., 1986, The St George Group (Lower Ordovician) of western Newfoundland: tidal flat island model for carbonate sedimentation in shallow epeiric seas: Sedimentology, v. 33, p. 313–343.

Puga-Bernabéu, A., Braga, J., and Martin, J., 2007, High-frequency cycles in Upper-Miocene ramp-temperate carbonates (Sorbas Basin, SE Spain): Facies, v. 53, p. 329–345.

Puga-Bernabéu, Á., Martín, J.M., Braga, J.C., and Aguirre, J., 2014, Offshore remobilization processes and deposits in low-energy temperate-water carbonate-ramp systems: examples from the Neogene basins of the Betic Cordillera (SE Spain): Sedimentary Geology, v. 304, p. 11–27.

Rankey, E.C., Bachtel, S.L., and Kaufman, J., 1999, Controls on stratigraphic architecture of icehouse mixed carbonate–siliciclastic systems: a case study from the Holder Formation (Pennsylvanian, Virgillan), Sacramento Mountains, New Mexico, *in* Harris, P. M., and Simo, J.A., eds., Advances in Carbonate Sequence Stratigraphy: Application to Reservoirs, Outcrops and Models: SEPM, Special Publication 63, p. 127–150.

Razin, P., Taati, F., and Van Buchem, F.S.P., 2010, Sequence stratigraphy of Cenomanian–Turonian carbonate platform margins (Sarvak Formation) in the High Zagros, SW Iran: an outcrop reference model for the Arabian Plate, *in* Van Buchem, F.S.P., Gerdes, K.D., and Esteban, M., eds., Mesozoic and Cenozoic Carbonate Systems of the Mediterranean and the Middle East: Stratigraphic and Diagenetic Reference Models: Geological Society of London, Special Publication 329, p. 187–218.

Reijmer, J.J., 2021, Marine carbonate factories: review and update: Sedimentology, v. 68, p. 1729–1796.

Reuter, M., and Brachert, T., 2007, Freshwater discharge and sediment dispersal: control on growth, ecological structure, and geometry of Late Miocene shallow-water coral ecosystems (Early Tortonian, Crete–Greece): Palaeogeography, Palaeoclimatology, Palaeoecology, v. 255, p. 308–328.

Riaza, C., and Martinez del Olmo, W., 1996, Depositional model of the Guadalquivir–Gulf of Cadiz Tertiary basin, *in* Friend, P.F., and Dabrio, C., eds., Tertiary Basins of Spain: The Stratigraphic Record of Crustal Kinematics: Cambridge University Press, p. 330–338.

Riding, R., Braga, J.C., Martin, J.M., and Sánchez-Almazo, I.M., 1998, Mediterranean Messinian Salinity Crisis: constraints from a coeval marginal basin, Sorbas, southeastern Spain: Marine Geology, v. 146, p. 1–20.

Riegl, B., 2001, Inhibition of reef framework by frequent disturbance: examples from the Arabian Gulf, South Africa, and the Cayman Islands: Palaeogeography, Palaeoclimatology, Palaeoecology, v. 175, p. 79–101.

Rodriguez-Fernandez, J., Azor, A., and Azanon, J.M., 2012, The Betic intramontane basins (SE Spain): stratigraphy, subsidence, and tectonic history, *in* Busby, C., and Azor, A., eds., Tectonics of Sedimentary Basins: Recent Advances: Blackwell Publishing, p. 461–479.

Rosleff-Soerensen, B., Reuning, L., Back, S., and Kukla, P., 2012, Seismic geomorphology and growth architecture of a Miocene barrier reef, Browse Basin, NW-Australia: Marine and Petroleum Geology, v. 29, p. 233–254.

Rouchy, J.M., Taberner, C., Blanc-Valleron, M.-M., Sprovieri, R., Russell, M., Pierre, C., Di Stefano, E., Pueyo, J.J., Caruso, A., Dinarès-Turell, J., Gomis-Coll, E., Wolff, G.A., Cespuglio, G., Ditchfield, P., Pestrea, S., Combourieu-Nebout, N., Santisteban, C., and Grimalt, J.O., 1998, Sedimentary and diagenetic markers of the restriction in a marine basin: the Lorca Basin (SE Spain) during the Messinian: Sedimentary Geology, v. 121, p. 23–55.

Ruchonnet, C., and Kindler, P., 2010, Facies models and geometries of the Ragusa Platform (SE Sicily, Italy) near the Serravallian–Tortonian boundary, *in* Mutti, M., Piller, W., and Betzler, C., eds., Carbonate Systems during the Oligocene–Miocene Climatic Transition: International Association of Sedimentologists, Special Publication 42, p. 71–88.

Sælen, G., Lunde, I.L., Porten, K.W., Braga, J., Dundas, S.H., Ninnemann, U.S., Ronen, Y., and Talbot, M.R., 2016, Oyster shells as recorders of short-term oscillations of salinity and temperature during deposition of coral bioherms and reefs in the Miocene Lorca Basin, SE Spain: Journal of Sedimentary Research, v. 86, p. 637–667.

Saint-Martin, J.P., and Rouchy, J.M., 1990, The Messinian carbonate platforms in the western Mediterranean: their importance for the reconstruction of the late Miocene sea-level variations: Société Géologique de France, Bulletin, v. 8, p. 83–94.

Sanz de Galdeano, C., 1990, Geologic evolution of the Betic Cordilleras in the Western Mediterranean, Miocene to the present: Tectonophysics, v. 172, p. 107–119.

Sanz de Galdeano, C., and Vera, J.A., 1992, Stratigraphic record and palaeogeographical context of the Neogene basins in the Betic Cordillera, Spain: Basin Research, v. 4, p. 21–36.

Schäfer, P., Fortunato, H., Bader, B., Liebetrau, V., Bauch, T., and Reijmer, J., 2011, Growth rates and carbonate production by coralline red algae in upwelling and non-upwelling settings along the Pacific coast of Panama: Palaios, v. 26, p. 420–432.

Schlager, W., 2003, Benthic carbonate factories of the Phanerozoic: International Journal of Earth Sciences, v. 92, p. 445–464.

Schlager, W., 2005, Carbonate Sedimentology and Sequence Stratigraphy: SEPM, Concepts in Sedimentology and Paleontology 8, 200 p.

Schlager, W., and Warrlich, G., 2009, Record of sea-level fall in tropical carbonates: Basin Research, v. 21, p. 209–224.

Schwarz, E., Veiga, G.D., Álvarez Trentini, G., Isla, M.F., and Spalletti, L.A., 2018, Expanding the spectrum of shallow-marine, mixed carbonate–siliciclastic systems: processes, facies distribution and depositional controls of a siliciclastic-dominated example: Sedimentology, v. 65, p. 1558–1589.

Stow, D.A., and Shanmugam, G., 1980, Sequence of structures in fine-grained turbidites: comparison of recent deep-sea and ancient flysch sediments: Sedimentary Geology, v. 25, p. 23–42.

Targhi, S., Barhoun, N., Taoufiq, N.B., Achab, M., Salem, A.A., and Yousfi, M.Z., 2021, Vegetation climate and marine environmental reconstruction in the western Mediterranean (southern Rifian corridor, Morocco) over the Tortonian–Messinian transition: Heliyon, v. 7, doi:10.1016/j.heliyon.2021.e08569.

Thrana, C., and Talbot, M.R., 2006, High-frequency carbonate–siliciclastic cycles in the Miocene of the Lorca Basin (Western Mediterranean, SE Spain): Geologica Acta, v. 4, p. 343–354.

Tomassetti, L., and Brandano, M., 2013, Sea level changes recorded in mixed siliciclastic–carbonate shallow-water deposits: the Cala di Labra Formation (Burdigalian, Corsica): Sedimentary Geology, v. 294, p. 58–67.

Vecsei, A., 2004, Carbonate production on isolated banks since 20 k.a. BP: climatic implications: Palaeogeography, Palaeoclimatology, Palaeoecology, v. 214, p. 3–10.

Vennin, E., Rouchy, J.M., Chaix, C., Blanc-Valleron, M.M., Caruso, A., and Rommevau, V., 2004, Paleoecological constraints on reef-coral morphologies in the Tortonian–Early Messinian of the Lorca Basin, SE Spain: Palaeogeography, Palaeoclimatology, Palaeoecology, v. 213, p. 163–185.

Vieira, F.V., Bastos, A.C., Quaresma, V.S., Leite, M.D., Costa, A., Jr., Oliveira, K.S., Dalvi, C.F., Bahia, R.G., Holz, V.L., Moura, R.L., and Amado Filho, G.M., 2019, Along-shelf changes in mixed carbonate–siliciclastic sedimentation patterns: Continental Shelf Research, v. 187, doi:10.1016/j.csr.2019.103964

Warrlich, G., Bosence, D., and Waltham, D., 2005, 3D and 4D controls on carbonate depositional systems: sedimentological and sequence stratigraphic analysis of an attached carbonate platform and atoll (Miocene, Níjar Basin, SE Spain): Sedimentology, v. 52, p. 363–389.

Webster, J., Clague, D., Riker-Coleman, K., Gallup, C., Braga, J., Potts, D., Moore, J., Winterer, E., and Paull, C., 2004, Drowning of the −150 m reef off Hawaii: a casualty of global meltwater pulse 1A?: Geology, v. 32, p. 249–252.

Wilson, M., 2005, Development of equatorial delta-front patch reefs during the Neogene, Borneo: Journal of Sedimentary Research, v. 75, p. 114–133.

Wilson, M., and Lokier, S., 2002, Siliciclastic and volcaniclastic influences on equatorial carbonates: insights from the Neogene of Indonesia: Sedimentology, v. 49, p. 583–601.

Winsemann, J., Asprion, U., Meyer, T., and Schramm, C., 2007, Facies characteristics of Middle Pleistocene (Saalian) ice-margin subaqueous fan and delta deposits, glacial Lake Leine, NW Germany: Sedimentary Geology, v. 193, p. 105–129.

Winsemann, J., Hornung, J. J., Meinsen, J., Asprion, U., Polom, U., Brandes, C., Bußmann, M., and Weber, C., 2009, Anatomy of a subaqueous ice-contact fan and delta complex, Middle Pleistocene, North-west Germany: Sedimentology, v. 56, p. 1041–1076.

Wright, V.P., and Burgess, P.M., 2005, The carbonate factory continuum, facies mosaics and microfacies: an appraisal of some of the key concepts underpinning carbonate sedimentology: Facies, v. 51, p. 17–23.

Wrobel, F., and Michalzik, D., 1999, Facies successions in the pre-evaporitic Late Miocene of the Lorca Basin, SE Spain: Sedimentary Geology, v. 127, p. 171–191.

Yamano, H., Hori, K., Yamauchi, M., Yamagawa, O., and Ohmura, A., 2001, Highest-latitude coral reef at Iki Island, Japan: Coral Reefs, v. 20, p. 9–12.

Yamano, H., Sugihara, K., Watanabe, T., Shimamura, M., and Hyeong, K., 2012, Coral reefs at 34 N, Japan: exploring the end of environmental gradients: Geology, v. 40, p. 835–838.

Zecchin, M., and Catuneanu, O., 2017, High-resolution sequence stratigraphy of clastic shelves VI: mixed siliciclastic–carbonate systems: Marine and Petroleum Geology, v. 88, p. 712–723.

Zeller, M., Verwer, K., Eberli, G.P., Massaferro, J.L., Schwarz, E., and Spalletti, L., 2015, Depositional controls on mixed carbonate–siliciclastic cycles and sequences on gently inclined shelf profiles: Sedimentology, v. 62, p. 2009–2037.

.